NASA TECHNICAL NOTE

NASA TN D-7178

NASA TN D-7178

HYPERVELOCITY IMPACT TESTING OF CABLES

by David W. Jex, Albert B. Adkinson, James E. English, and Carl E. Linebaugh

George C. Marshall Space Flight Center
Marshall Space Flight Center, Ala. 35812

NATIONAL AERONAUTICS AND SPACE ADMINISTRATION • WASHINGTON, D. C. • FEBRUARY 1973

1. Report No. NASA TN D-7178	2. Government Accession No.	3. Recipient's Catalog No.
4. Title and Subtitle Hypervelocity Impact Testing of Cables		5. Report Date February 1973 6. Performing Organization Code
7. Author(s) David W. Jex, Albert B. Adkinson,* James E. English,* and Carl E. Linebaugh*		8. Performing Organization Report No. M450 10. Work Unit No.
9. Performing Organization Name and Address George C. Marshall Space Flight Center Marshall Space Flight Center, Alabama 35812		11. Contract or Grant No. 13. Type of Report and Period Covered Technical Note
12. Sponsoring Agency Name and Address National Aeronautics and Space Administration Washington, D.C. 20546		14. Sponsoring Agency Code

15. Supplementary Notes

Prepared by Space Sciences Laboratory, Science and Engineering

*Employees of Sperry Rand Corporation

16. Abstract

This report presents the physics and electrical results obtained from simulated micrometeoroid testing of certain Skylab cables. The test procedure, electrical circuits, test equipment, and cable types utilized are also explained.

17. Key Words (Suggested by Author(s))	18. Distribution Statement		
19. Security Classif. (of this report) Unclassified	20. Security Classif. (of this page) Unclassified	21. No. of Pages 59	22. Price* $3.00

* For sale by the National Technical Information Service, Springfield, Virginia 22151

EDITORS NOTE

Use of trade names or names of manufacturers in this report does not constitute an official endorsement of such products or manufacturers, either express or implied, by the National Aeronautics and Space Administration or any other agency of the United States government.

TABLE OF CONTENTS

LIST OF ILLUSTRATIONS

LIST OF ILLUSTRATIONS (Continued)

LIST OF TABLES

HYPERVELOCITY IMPACT TESTING OF CABLES

SUMMARY

The hypervelocity impact tests were performed to gain information that can be used to evaluate the anticipated damage to cabling and cable-connected systems that are exposed to the meteoroid environment.

The data from direct impacts have bracketed the failure point for certain type cables. The data for indirect impacts should be used with caution after reading this report.

The following tabulation summarizes the results:

	End View of Cable Types	Direct Impacts, Energy Necessary for Failure (J)	Indirect Impacts, Energy Necessary for Failure (J)	Physical Description of Failure Mode
Type 1	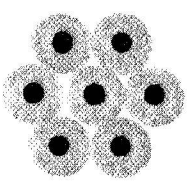	8.64 to 11.00	845 to 1172	Conductor cable severed or broken Excessive insulation stripped away
Type 2	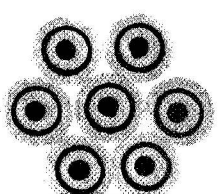	0.164 to 0.210	630 to 678	Short of center conductor to ground shield
Type 3	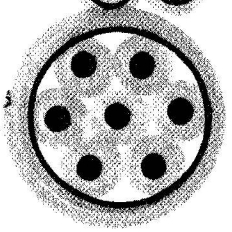	2.03 to 2.62		Short of center conductor to ground shield
Type 5	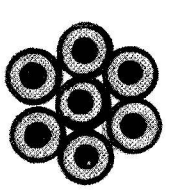	10.2 to 11.4	–	Conductor severed or broken

	End View of Cable Types	Direct Impacts, Energy Necessary for Failure (J)	Indirect Impacts, Energy Necessary for Failure (J)	Physical Description of Failure Mode
Type 7		2.68 to 5.68 0.0595-cm-diameter glass spheres (ρ = 2.5 g/cm^3)		Conductor severed or broken

 Insulation

 Conductor

INTRODUCTION

Insulated cabling represents a fire hazard if it is contained inside the pressure wall of a spacecraft. Therefore, where possible, for Skylab and other spacecraft, all the cabling is placed outside the pressure wall. This location exposes the cables to the meteoroid environment. Most Apollo Telescope Mount (ATM) cables are also exposed to direct and indirect meteoroid impacts. An indirect impact is one in which a meteoroid impacts a bumper or shield with sufficient energy to penetrate it and generate debris that will encounter the cabling behind this shield or bumper. A direct impact is one in which the meteoroid itself impacts the cabling.

Very little information was available to assess the effects of this environment. Therefore, it was necessary to generate sufficient information to determine if additional cable protection was necessary to stay within the mission constraint probability.

It was obvious that a complete definition of all the parameter relationships in the time available was impossible. Therefore, the approach was to select some given parameters and perform experiments to acquire basic data. To acquire the basic data, a mutual effort was established between Astronautics (ASTN), Astrionics (ASTR), and Space Sciences Laboratories (SSL) of MSFC. The electrical configuration, circuits, currents, etc., were determined by ASTR. The mass and impact probability of meteoroids to be simulated was determined by SSL and ASTN. The compilation, accumulation, and evaluation of the data were made by SSL and the Sperry Rand Corporation support personnel working for ASTR. The light gas-gun facility at SSL was used for the simulated impacts because of its unique capabilities. The information derived was sent to Clyde Nevins, ASTN, who is responsible for final recommendations affecting the Skylab meteoroid protection.

I. PHYSICS

The objective of the test series was to determine the ballistic limit or failure point for each type of cable tested. The ballistic limit or failure point was determined by

bracketing; i.e., the parameter representing the potential damage capability of the impacting projectile was ranked in order from lowest to highest value. Then, moving from the low values, which did not cause failure, to the high values, which did cause failure, a bracket around the actual ballistic limit was established.

The ballistic limit was defined as the case where the cable failed to perform its proper function. There are two general ways in which this could occur: (1) if the cable was shorted to another conductor, and (2) if the cable were broken or severed.

The parameter used to represent the potential damage capability of the impacting projectile is the energy. Energy extrapolation is conservative, as shown in the following discussion.

A. Energy Extrapolation Discussion

The meteoroid environment model [1, 2] is a meteoroid mass-flux curve given in terms of the number of meteoroids of mass (m) or greater that will impact 1 m^2/s versus the meteoroid mass (m). The data plotted are from Pegasus spacecraft, Explorer XVI and XXIII spacecraft, Gemini window evaluation, and photographic meteor observations.

The velocity of a meteoroid of mass (m) is assumed to be 20 km/s. Its density is assumed to be 0.5 g/cm^3. The laboratory simulation in this test series had an average velocity of 6 km/s using glass spheres of density 2.5 g/cm^3.

When a ballistic limit is established using laboratory techniques, how can the information be extrapolated with confidence to the meteoroid values?

Reference 3 describes the tests used in calibrating the Pegasus and Explorer XXIII detection panels. These detectors were used to define the meteoroid environment model in References 1 and 2. In this publication, a well-established penetration formula is presented:

$$T = K(p)^{0.148}(m)^{0.352}(v)^{0.875}$$

where

T = target thickness that will be penetrated (cm)

K = target material constant = $\dfrac{0.816}{(\epsilon)^{1/18}(P_T)^{1/2}}$

p = projectile density

m = projectile mass

v = projectile velocity.

ϵ = ductility (percent elongation)

P_T = target density.

Assuming this formula is valid, two projectiles represent the same potential damage, as far as penetration is concerned, if

$$p_1^{0.148}\ m_1^{0.352}\ v_1^{0.875} = p_2^{0.148}\ m_2^{0.352}\ v_2^{0.875}$$

$$\left(\frac{m_1}{m_2}\right)^{0.352} = \left(\frac{p_2}{p_1}\right)^{0.148} \left(\frac{v_2}{v_1}\right)^{0.875}$$

by simple manipulation

$$m_1 = \left(\frac{p_2}{p_1}\right)^{0.420} \left(\frac{v_2}{v_1}\right)^{2.49} (m_2)$$

Substituting the laboratory and meteoroid values, the relationship, for this test series, between the laboratory mass (m_1) and its equivalent meteoroid mass (m_2) is obtained:

$$m_2 \approx 1/10\, m_1$$

Assuming energy extrapolation is valid, two projectiles represent the same potential damage, if

$$1/2\, m_1\, v_1^2 = 1/2\, m_2\, v_2^2$$

$$m_1 = (v_2/v_1)^2\, m_2$$

Again, substituting the respective values yields

$$m_2 \approx 1/11\, m_1$$

Thus, it is seen that energy extrapolation for this test series is conservative. The tables are, therefore, presented in terms of energy for the convenience of the user.

A more detailed description of the physical phenomena is of interest for understanding the data obtained for predicting effects on other types of cables and is given in the following section.

B. Physical Phenomena of Hypervelocity Impact

Many complex events occur in a hypervelocity impact. Rather than discussing details, the explanation here will deal with basic concepts so that a general understanding can be developed. The details will be left to in-depth publications already available.

One of the characteristics of a hypervelocity impact of two materials is that a shock wave will be generated at the interface and proceed into the respective materials with a velocity (D) equal to or faster than the sound velocity (C) in the material. The volume of material directly behind the shock wave is compressed. The material in front is undisturbed.

The process can be described in two reference systems: (1) a system in which the undisturbed material is at rest and the compressed material is moving, or (2) a system in which the undisturbed material is moving and the compressed material is at rest. These two systems of reference are shown to be equivalent in Figure 1. Velocities D and U have the same value in both systems; however, it should be noted that the velocity of the shock wave is defined differently in the two systems. This difference is because of the manner in which D is defined. It is defined as the velocity of the shock wave with respect to the undisturbed material.

Since release waves that travel at the sound velocity (C) of the material will be discussed, it should be noted that the sound velocity in the undisturbed material is not the same as the sound velocity in the compressed material. The release wave will always travel faster in the compressed material; therefore, an equation of state is necessary to define the desired parameters and velocities. Suffice it to say that the release waves releases the compressed material and is generated from a free surface and/or discontinuity. For the following discussion, assume that the released material is fragmented.

Assume that an incompressible cylindrical projectile impacts a compressible target material and that the only free surface is the rear of the target. Figure 2A illustrates the process as a function of time.

The scaling factors used in each illustration of Figure 2 are that: (1) material can be compressed to one-half its original volume, (2) the shock wave travels 2X for each time increment, and (3) the release wave travels 3X for each time increment.

Reverse the situation in Figure 2A and assume that a compressible cylindrical projectile impacts an incompressible target. This time, the only free surfaces are the ends of the projectile. Remove the incompressible target after five time increments, as shown in Figure 2B. When this happens, the release wave will begin at the original interface between the two materials. The shock wave will proceed until the release wave overtakes and releases it.

Combine these two processes, as in Figure 2C. In addition to both materials being compressible, both have an equal velocity toward each other, and the original interface is stationary. The process illustrates that when a traveling projectile impacts a material, the impact parameters and the ratio between the length of the projectile and the thickness of

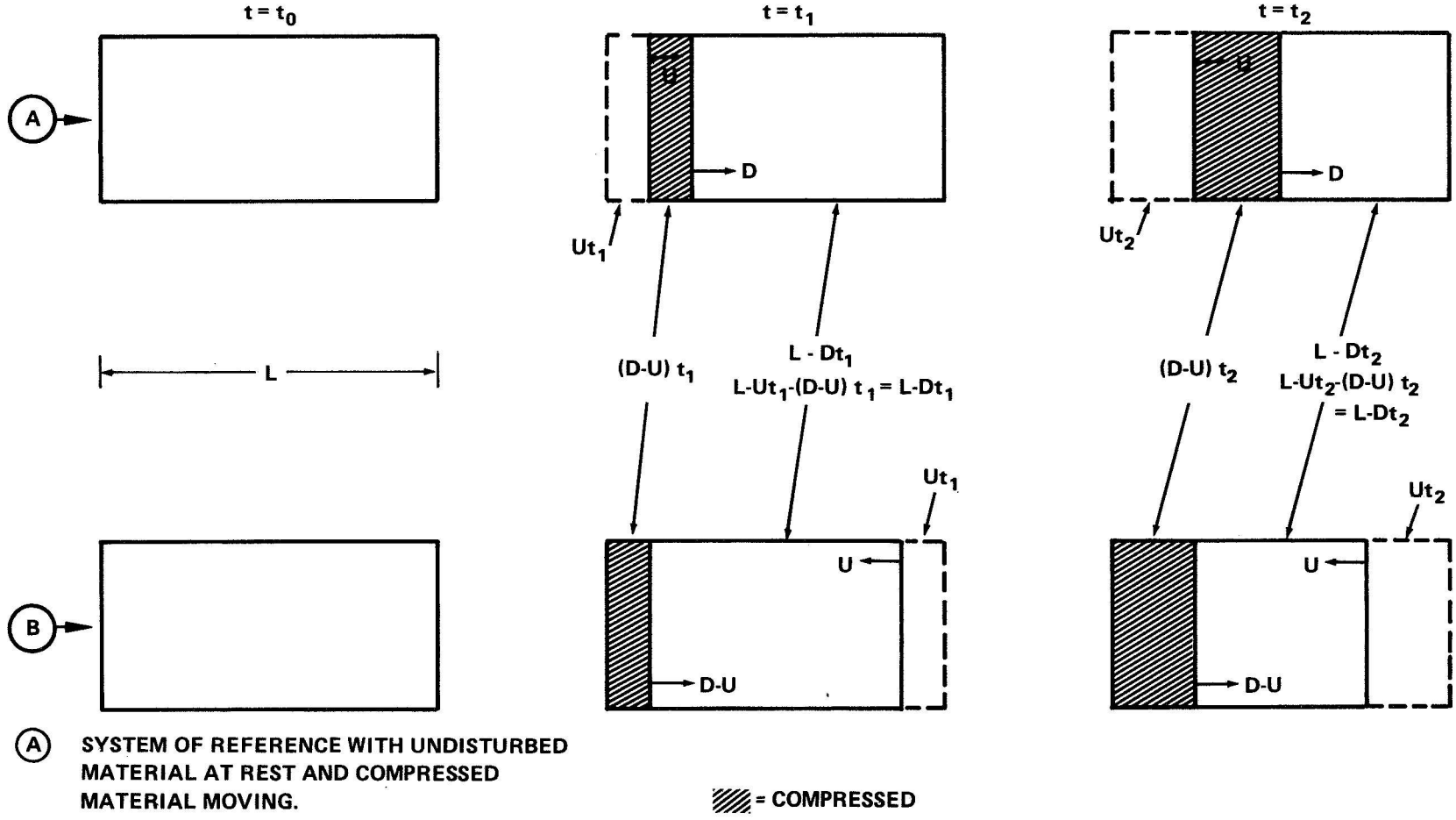

(A) SYSTEM OF REFERENCE WITH UNDISTURBED MATERIAL AT REST AND COMPRESSED MATERIAL MOVING.

(B) SYSTEM OF REFERENCE WITH UNDISTURBED MATERIAL MOVING AND COMPRESSED MATERIAL AT REST.

Figure 1. Equivalent reference systems.

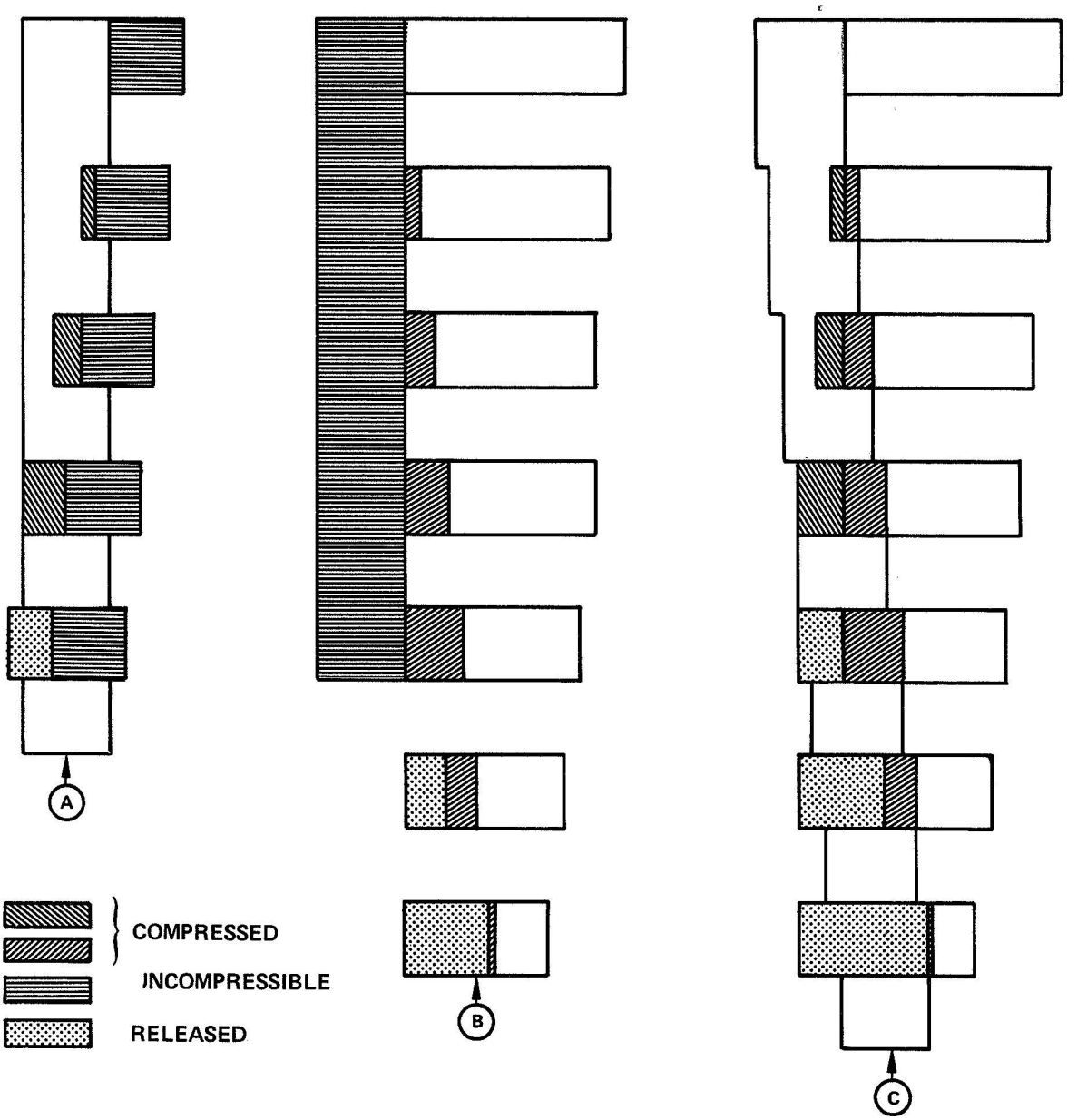

Figure 2. Shocked material – Released material relationship for (a) compressible target, incompressible projectile; (b) incompressible target, compressible projectile; and (c) compressible target, projectile where the shock wave travels at 2X and the release wave travels at 3X.

the target material determine if the original projectile is totally fragmented or if part of it will proceed at its original velocity through a hole generated in the target by the impact phenomena.

The fragmentation process can be understood by visualizing a group of billiard balls connected to each other by springs. A compressive force acting on the group will force them closer together, storing energy in the springs. There is a point at which the restoring force will balance the compressive force. This state would be the compressed state of the group under the given force. When the compressive force is removed, the springs will turn the stored energy into kinetic energy and accelerate the balls toward the original equilibrium configuration. Depending on the energies involved and the strength of the springs, the end result would be any one of three conditions: (1) the group is restored, after some oscillation, to its original configuration, (2) some of the springs are stretched beyond their elastic limit and the group returns to its original configuration with some distortions, and/or (3) some springs are broken and the group is fragmented.

This simple approach in describing the fragmentation phenomena has assumed that the fragmentation will be uniform; i.e., each "chunk" of debris will be the same, whereas in reality the debris particles vary in size and trajectory. The concept, however, will be useful in understanding what is taking place.

Figures 3 and 4 are plots of the impact processes already discussed using parameters obtained from the equation of state for an aluminum-on-aluminum impact calculated by Naumann[4]. These figures assume the stationary interface reference system where the target and projectile approach each other at equal velocities. The initial time ($t = 0$) is the moment of contact between the two materials. The time axis represents the stationary interface with the rear surface of the target and projectile approaching it as a function of time.

The shock wave begins at the interface (0,0) and travels in both materials toward the approaching rear surfaces at an equal velocity. As the shock wave reaches the rear surface, the release wave is generated and travels in an opposite direction at a higher velocity.

In Figure 3, the release wave does not overtake the shock wave in the projectile until the entire length of projectile is processed and, therefore, as illustrated in the pictorial representation at the bottom, the entire projectile is fragmented.

In Figure 4, the release wave overtakes the shock wave in the projectile and releases it, allowing a piece of the projectile to continue at its original velocity through the hole generated in the target plate by the impact phenomena.

This simplified explanation of the physical phenomena of hypervelocity impact does not contain an explanation for many complex interactions which occur, but it does present the concepts necessary in discussing some of the effects observed when the cables were examined.

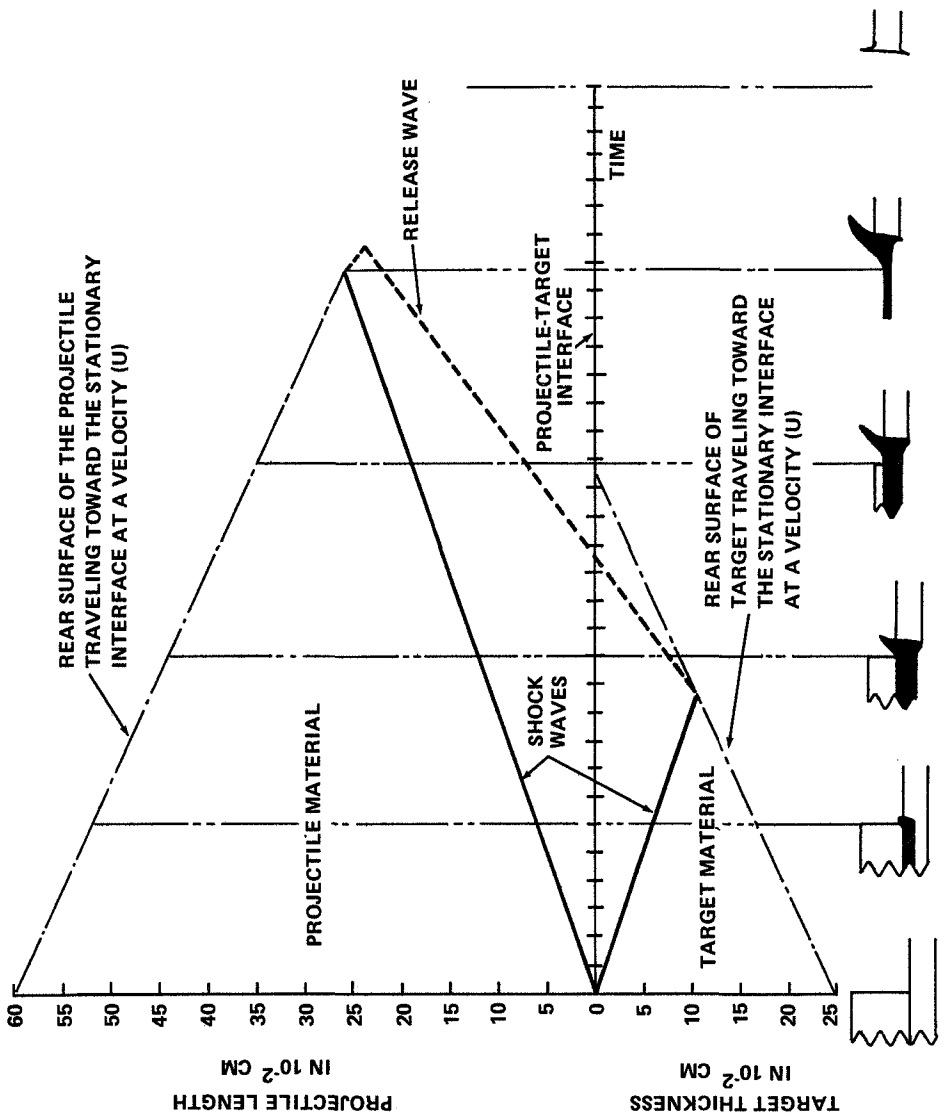

Figure 3. Aluminum on aluminum impact where the release wave does not overtake the shock wave until the projectile is completely processed. (Therefore, there is complete fragmentation of the projectile.)

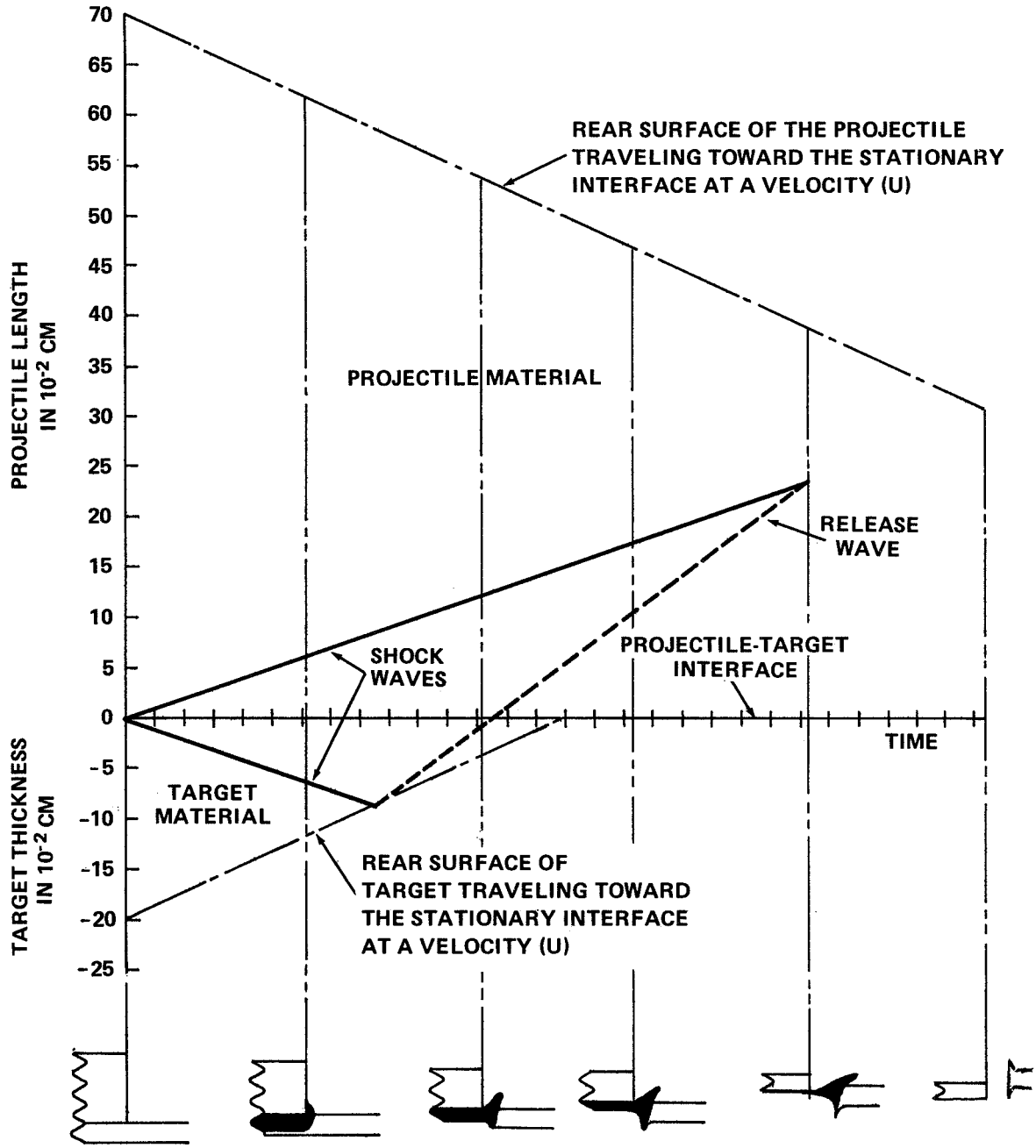

Figure 4. Aluminum on aluminum impact where the release wave overtakes the shock wave before the projectile is completely processed. (Therefore, there is a part of the projectile which proceeds at the initial velocity through the hole created in the target.)

C. Explanation of Physical Examination of Impacted Cables

Two types of impacts were investigated: direct and indirect. Direct impacts are those where projectiles of a knowr size d velocity encounter the cables directly. Indirect impacts are those where projectiles of a known size and velocity impact a thin bumper material causing fragmentation, as discussed in the previous section. This indirect impact produces fragments or debris particles of unknown size and velocity which impact the cables.

1. Direct Impacts. Tests on the unshielded cables type 1 had some common characteristics. The impact shocked the insulation material. The free surfaces allowed the total release wave to separate part of this material from the inner conductor and the rest of the insulation material. The result was that an area of the cabling was left with no insulating material to protect the conductor from exposure. In many cases, additional damage to the inner conductor was done by the part of the projectile that was not fragmented passing through this vacated area and encountering the metal strands.

All impacts were in the hypervelocity region; therefore, a plasma was created. When the impact affected only one wire, no shorting was monitored because there was no completed circuit path. However, when the impact affected two adjacent wires of different potential, a short would originate and continue until the plasma dissipated, at which time the short would terminate. It was found that the typical length of time for this type of short was 10 to 50 μs.

Shorts of this duration were not considered failures. Therefore, the size of the particles was increased until the wires were actually severed. This, of course, made the wires incapable of performing their normal function and was considered a failure. Typical examples of these impacts are shown in Figure 5.

Tests on the single shielded wire type 2 had characteristics that were different from the unshielded wire. In this case, the impact removed insulation as before, but all of the shorts monitored were at least 1000 μs in duration. Obviously, the plasma would generate a short of the same duration as before, and possibly longer, because of the smaller distance between the conductor and the grounded shield, but it would not generate a short two orders of magnitude longer. Therefore, the longer duration shorts need a different explanation.

It was found that the impact phenomena caused strands of the shielding to break and bend inward toward the center conductor. There was evidence of burning or arcing; consequently, this indicates that the impact phenomena caused broken strands of the shield to come in contact with the inner conductor and remain shorted until this path was burned free. This process could last for several hundreds of microseconds. It was concluded that this would explain the observed characteristics. In this case, a projectile needed to impact only one cable to fail because the path could be completed to ground through the shield on the same wire. Typical examples are shown in Figure 6.

Tests on the overall-shielded cables type 3 showed characteristics similar to the individually shielded cables; therefore, the explanation is essentially the same.

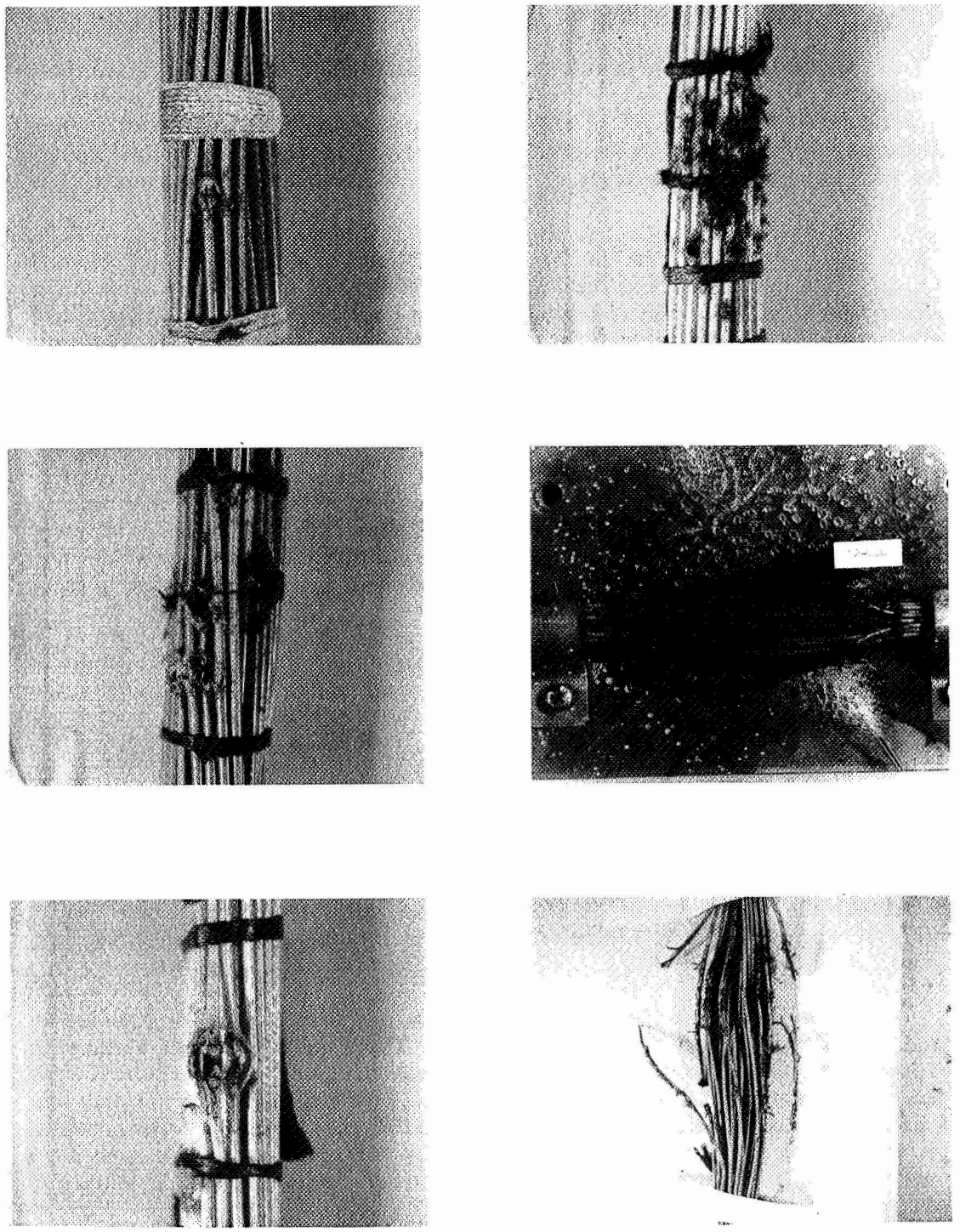

Figure 5. Typical impacts on cable type 1.

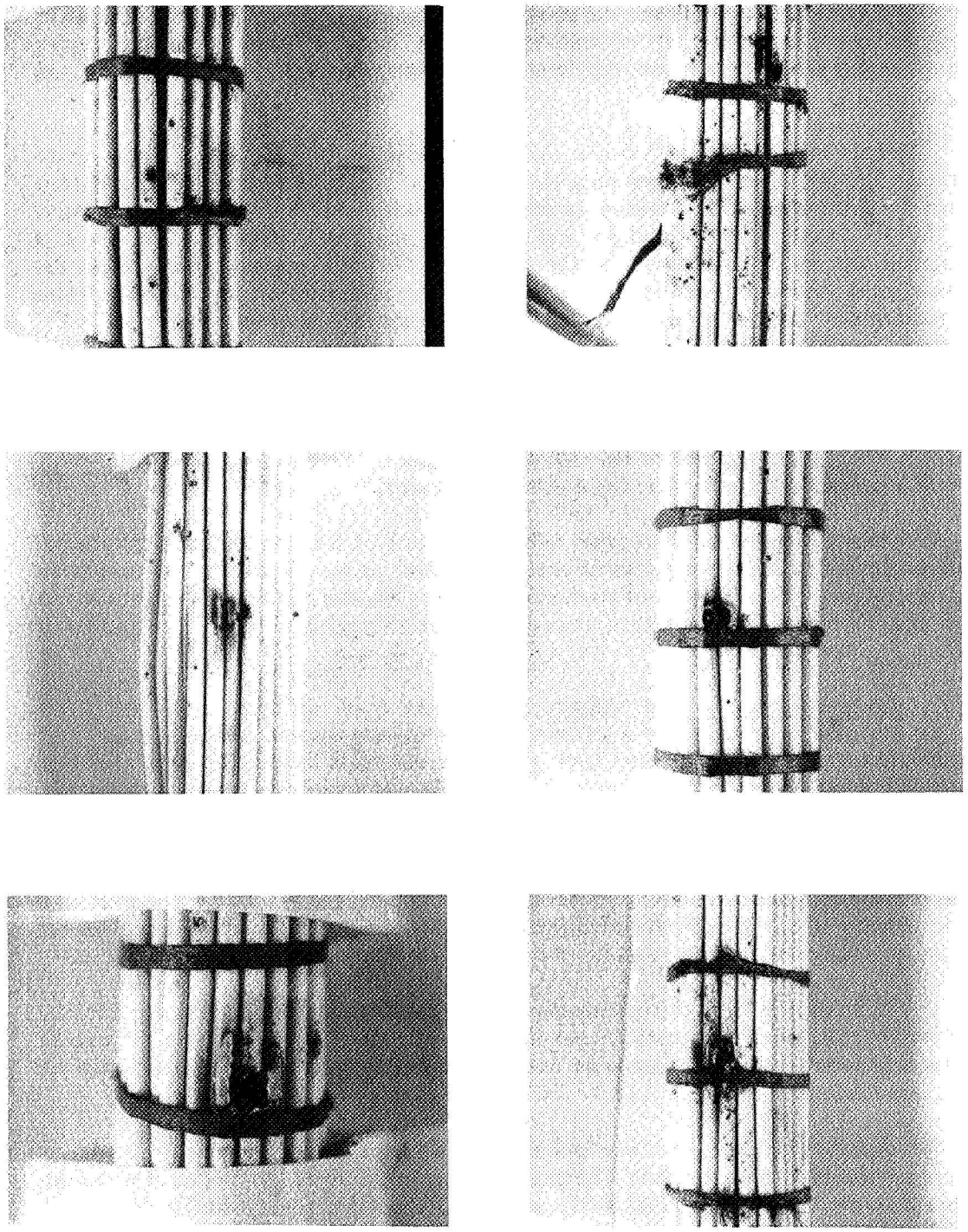

Figure 6. Typical impacts on cable type 2.

Examination of the coaxial cable type 5 showed evidence that the strands of shielding, broken during impact of this cable, bent outward away from the center conductor. In this series, failure was the breaking or severing of the conductor rather than shorting to the ground shield.

The only difference, other than size, between types 2 and 5 is the extra insulation on the outside of the grounding shield on type 2 cable. It is, therefore, concluded that when the ground shield is confined or externally constrained from outward motion, it will be forced through the insulation and short to the inner conductor. When it is unconstrained, the initial process will be the same; i.e., the initial impact process severs the strand and forces it toward the inner conductor. However, as the impact proceeds, a portion of the insulation is turned into a plasma whose expansion will reverse the motion of the broken strand and bend it outward as it is found in the final state.

This theory is further substantiated by the description of failure for cable type 2 in Section III: "Physical damage to cables may be misleading since a shielded cable hit by small size pellets appears to be perfect except for a few minor pinholes. However, four shorts were found between shield and wire when tested."

The 32-conductor flat cable failed when one of the conductors was severed. The ballistic limit is defined in terms of energy; however, it was found that there was an obvious dependence on size or area of contact. Therefore, the size of the glass spheres is also given on the summary sheet. Typical impacts on cable types 3, 5, and 7 are shown in Figure 7.

2. Indirect Impacts. The indirect impacts are quite different from the direct impacts. In this case, a projectile of a known size and velocity impacts a 0.064-cm (25-mil) thick aluminum sheet, simulating the Skylab bumper, which is located 12.7 cm (5 in.) in front of the cabling. Debris particles or fragments of an unknown size, phase, distribution, and velocity are created. The debris particles travel toward and encounter the cabling.

Solid debris particles traveling in the hypervelocity range will damage the cables, as previously described under direct impacts. Liquid and plasma debris will affect the cabling in a manner not specifically investigated in this study. The damage described for indirect impacts is a combination of all three types of debris.

It is obvious from the examination of the cables used during these experiments that the number of impacting particles per unit area of cabling is greater, and the overall effect was that long sections of wire were exposed, rather than isolated areas as found on the direct impacts.

Another general effect was evident. The wires that were affected by the debris cloud were separated from each other. The more damage to the wire, the further it was from a neighboring wire. This suggests that a large amount of plasma is generated. The expansion of the plasma causes the wire to isolate itself from nearby material.

Since the size, phase, distribution, and velocity of the debris particles are unknown, data indicating that a cable did or did not fail on a given shot may not be

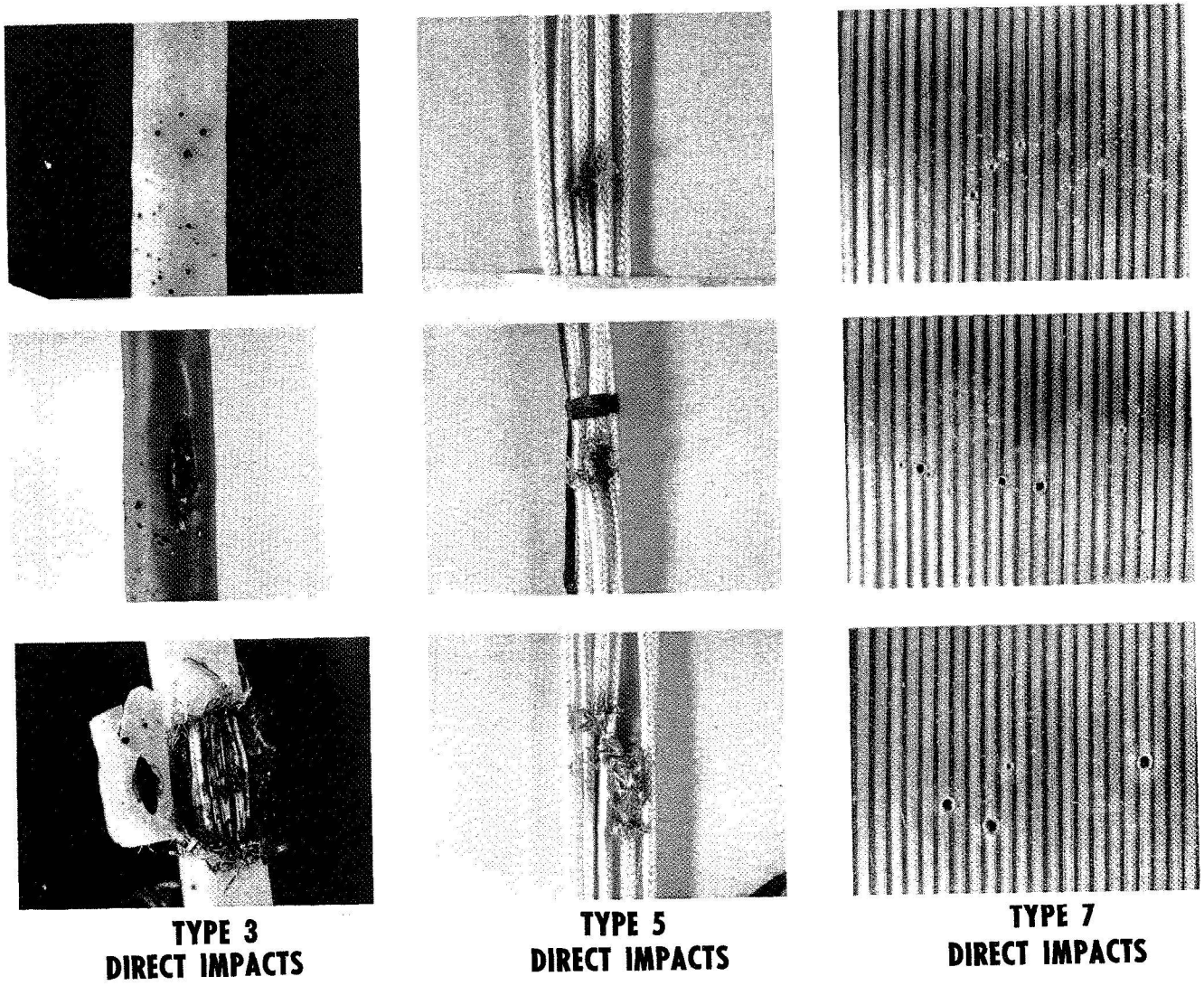

Figure 7. Typical impacts on cable types 3, 5, and 7.

consistent with another shot in the same test series because of the phase and distribution of particles that impact. Therefore, the data may appear ambiguous merely on the basis of probability. There was not enough time to conduct enough tests to eliminate this ambiguity. It was concluded that a decision on the amount of insulation removed from the wires made by visual inspection would define the failure point.

From this brief discussion, it should be apparent that the data on the indirect impacts may not be as reliable as the data on the direct impacts. Therefore, caution should be exercised when using these values.

3. Summary. The direct impacts of known particles at known velocities have bracketed the failure or break point of certain types of cabling.

The indirect impact data give "ballpark" figures for the failure or break point; but it should be remembered that the size, state, distribution, and velocities of the debris are not known and, therefore, a probability factor may be reflected.

II. ELECTRICAL ASPECTS

This section describes the electrical circuits and tests used in micrometeoroid testing of electrical cables. Testing was conducted according to Appendix A with the following deviations. Test sequences 5 and 6, 13 through 15, and 17 and 18 were not performed since these test sequences only required using different size wire. It was determined that no new information could be obtained from performing these tests; however, it was decided that since flat cable and coaxial cable are different type cables, tests using these two cables should be performed.

The cables used in these tests were representative of the majority of cables used on Skylab I. Cable type 1 was made of unshielded AWG 20 wire. Cable type 2 was made of single shielded AWG 20 wire. Cable type 3 was an overall shielded cable made of AWG 20 wire. Cable type 5 was a coaxial cable RG-179. Cable type 7 was 32-conductor flat cable.

Test specimen requirements such as lacing, cleaning, cable part numbers, mounting, etc., are found in Appendix A.

A. Electrical Circuitry

All circuits are basically the same as Figure 8, which is a detailed schematic of the test circuitry used. A description of this basic circuit is given, and only the essential differences in other test circuits are described. Figures 9 and 10 are simplified versions of Figure 8 with the appropriate cables used.

Each circuit was designed to allow for the detection of shorts and opens when the test specimen was bombarded by particles. The cables were constructed to allow half of the wires to complete a 30-volt circuit and the other half to complete a 60-volt circuit, resulting

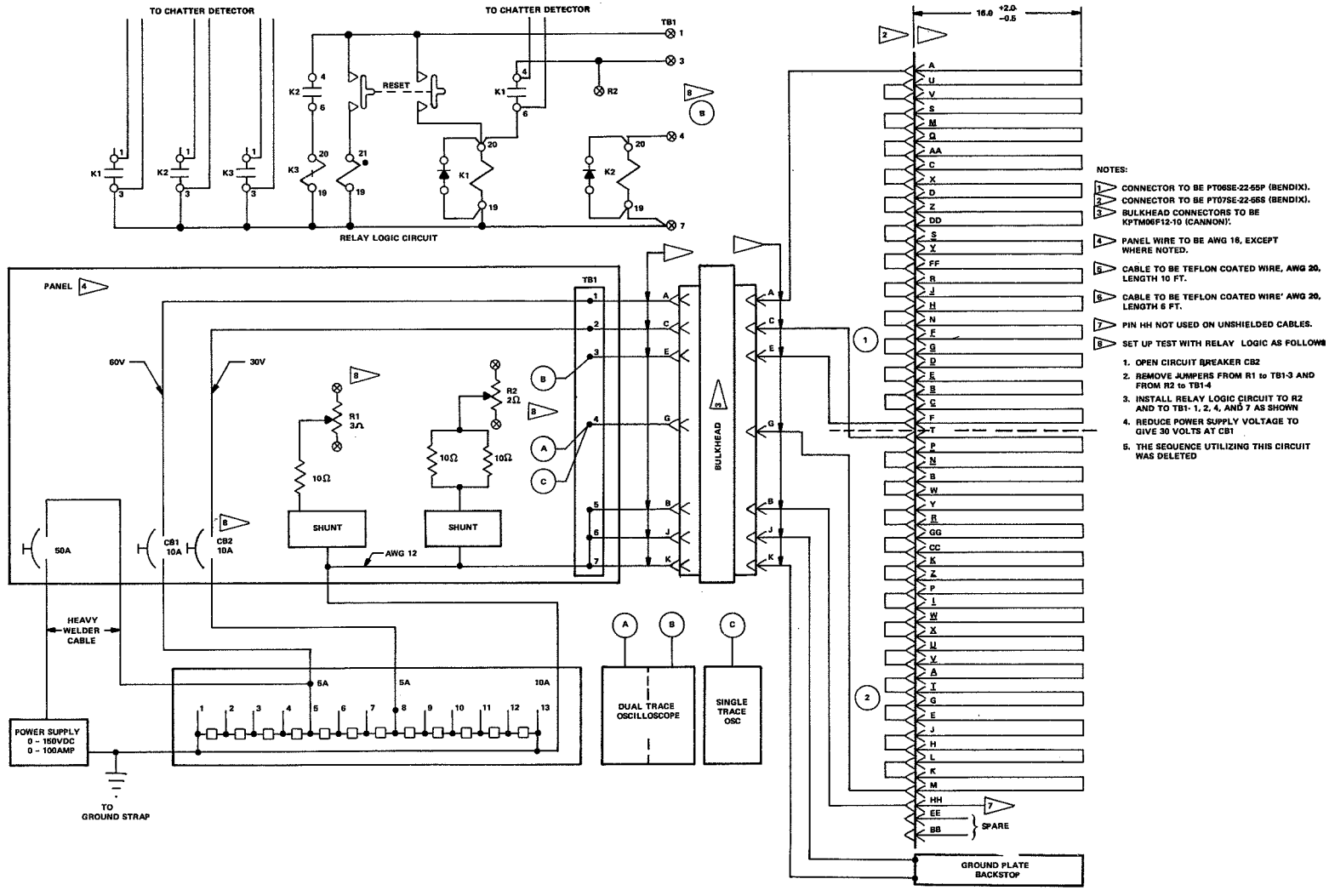

Figure 8. Micrometeoroid tester circuit diagram.

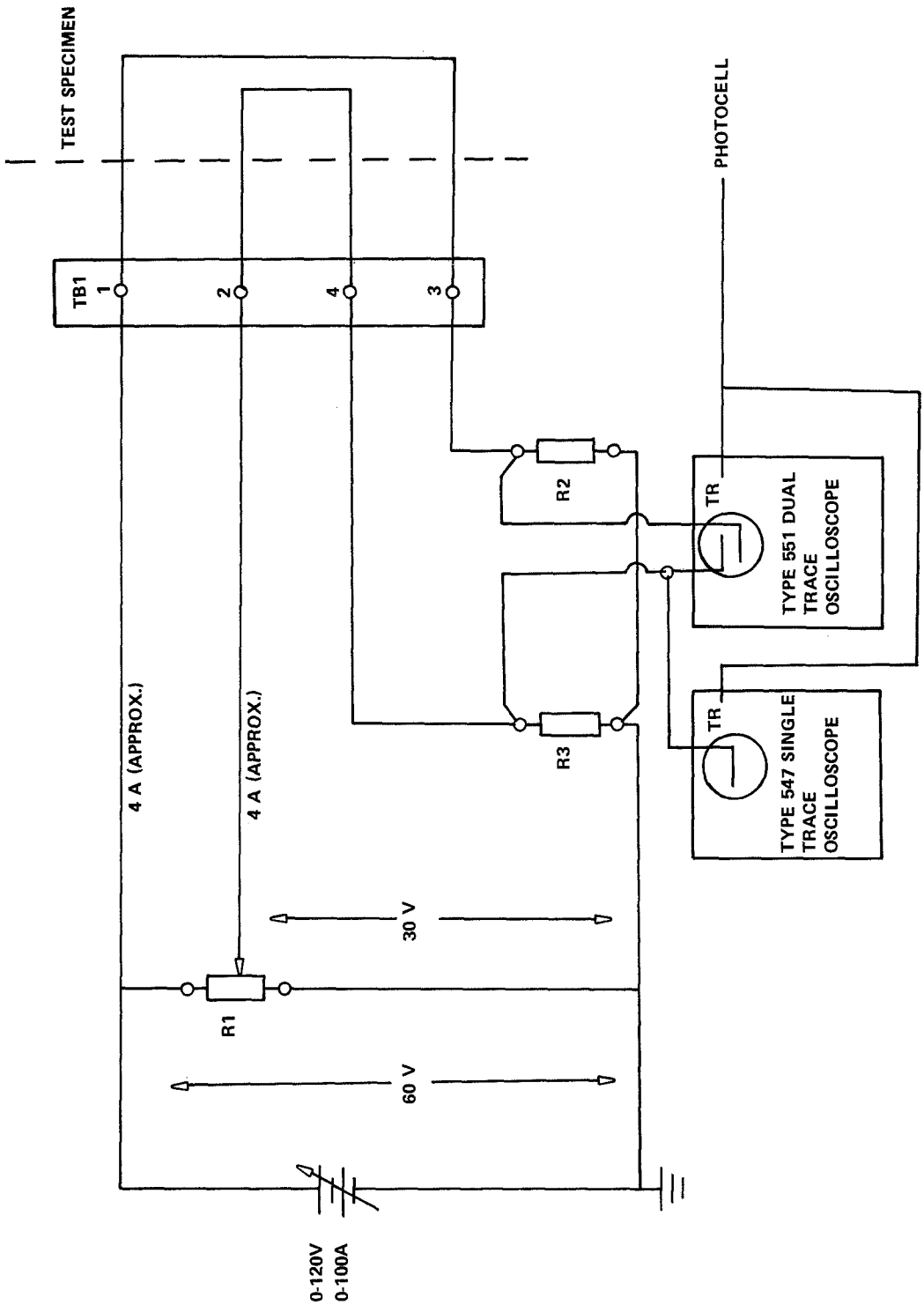

Figure 9. Test monitor circuit for cable type 1.

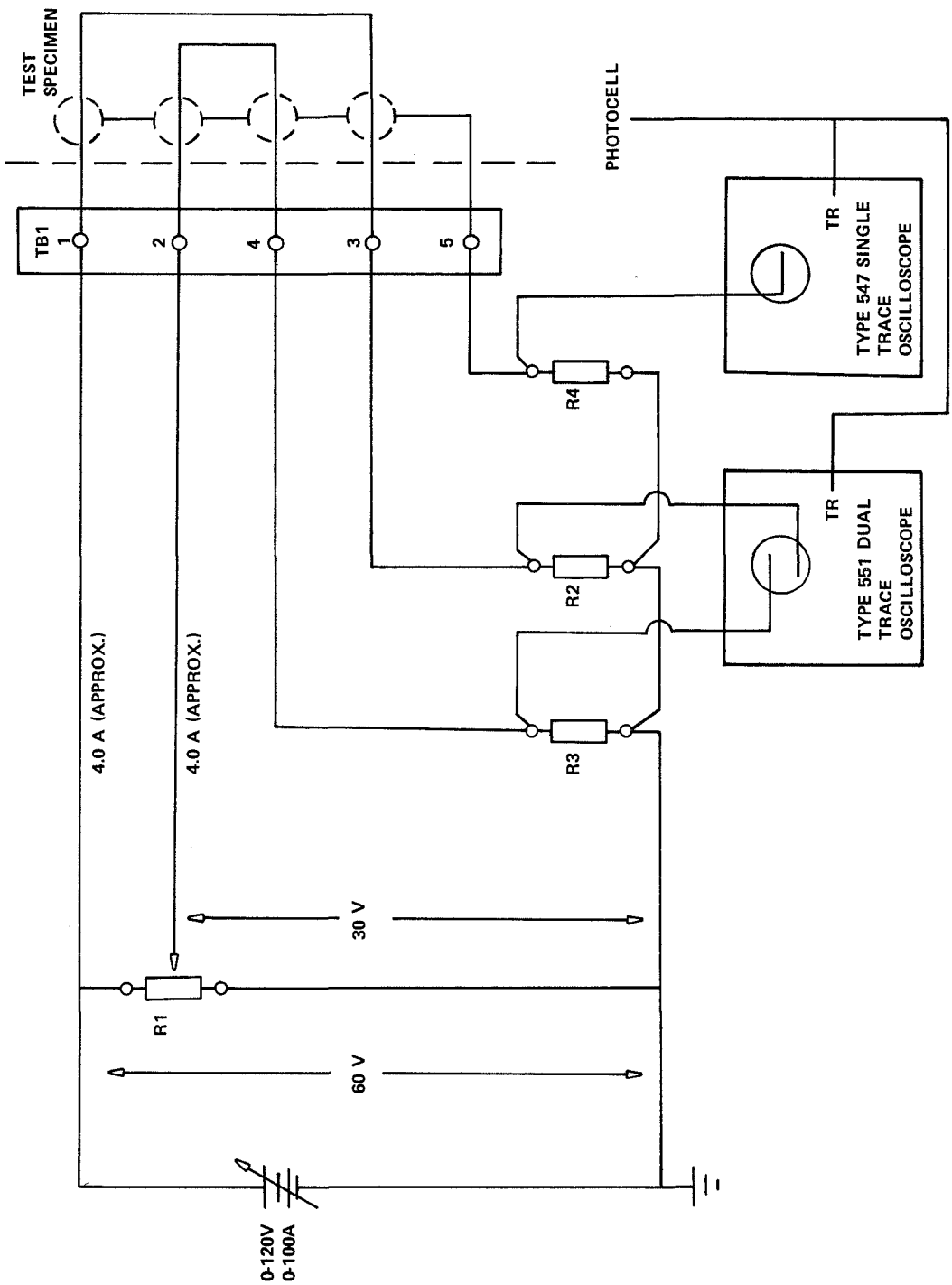

Figure 10. Test monitor circuit for cable types 2 and 3.

in a 30-volt difference to detect any shorts between wires. This was accomplished by using a large load bank, represented by terminals 1 through 13 in Figure 8, and by R1 in all other figures, and tapping off the desired voltage. The load bank also enabled the source to supply a large instantaneous current if and when the cables shorted. This is representative of the power supply used on Skylab I. In Figure 8, the current in each circuit was obtained by choosing appropriate value resistors, R1 and R3 in the 60-volt circuit and R2 and R4 in the 30-volt circuit. In Figures 9 and 10, this resistance is represented by R2 and R3. Each circuit was monitored by an oscilloscope which was triggered externally by a photocell, just prior to the particle hitting the cable. The circuit breakers were used to protect the power supply and electrical components.

Figure 9, which was used to test type 1 cables, functions exactly as Figure 8 describes.

Figure 10 differs slightly in that the test specimens used with this circuit were single shielded and overall shielded wire cable. Therefore, if either circuit shorted to the shield, the current would have a direct path to ground through the shield. To observe this, a small shunt, R4, was placed in the shield-to-ground line to permit monitoring of the line with an oscilloscope.

B. Fact Test

The purpose of this test was to determine the amount of damage caused by the micrometeoroid particles, and it was performed in two parts.

First, a continuity check was performed by running 4 amperes of current through the test specimen. A continuity check was then performed by applying 500 volts between each wire and ground to determine if the resistance was less than 100 MΩ. The fact machine printed out the discrepancies it found.

When testing began with the fact machine, the cables were checked at 1000 volts to detect a short less than 50 MΩ. This was changed beginning with test number 45 to agree with ATM wire specifications.

C. Leakage Test

The purpose of this test was to determine the amount of current required to open a short. The leakage tester is shown in Figure 11. Voltage was applied by the six-position switch. In the "off" position, if a direct short is present, the voltmeter will read the applied voltage. The switch was then varied through the six positions, putting a smaller value resistor in the circuit each time. All voltages were recorded. The voltage applied was increased until the short opened. A maximum of 45 volts can be applied to this circuit.

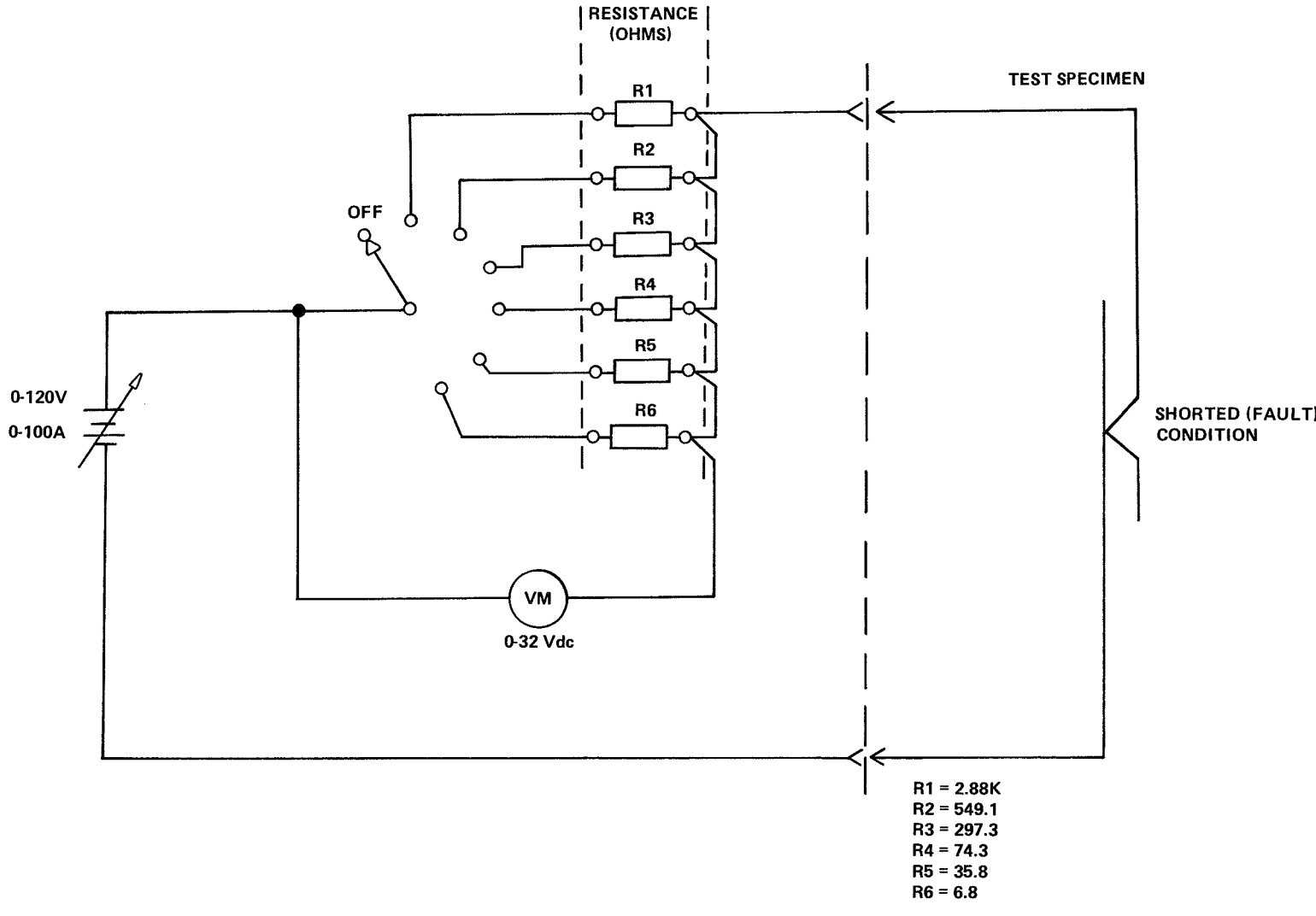

Figure 11. Test circuit for current leakage test.

D. Evaluation Test

This test consisted of counting the number of strands broken or otherwise damaged in the wire to determine if sufficient damage resulted from the firings to impair the current-carrying capability of the wire.

E. Conclusion

The circuits and test results were extremely informative; however, before the results are analyzed, a few points require clarification. The breakpoint was picked between the highest energy at which no failure occurred and the lowest energy at which failure did occur. Failure is defined as shorts or opens. A wire is classified as open if it was completely severed. However, three types of shorts may result from micrometeoroid bombardment.

The first type is a short caused by a particle hitting the cable. The shorted path is through the plasma and lasts until the plasma is dissipated. This type of short may cause an approximate 10- to 50-μs pulse.

The second type of short is one that remains after the plasma has dissipated, but opens or burns itself off after a short period of time. This type of short may last approximately 1000 μs or longer and is considered a failure since this period of time is of sufficient length that damage to electrical components may result.

The third type is a permanent short which remains after the plasma has dissipated and does not burn itself open.

For direct hits, it was determined that the data obtained were accurate; however, for indirect or bumper shots, the results were inconclusive. The reason for this was explained previously, and only the results obtained for direct hits are discussed in this section. Cable type 1 was classified as the least troublesome, and cable types 2 and 3 as the most problematic.

Type 1 is an unshielded cable. A total of 20 test firings (simulated micrometeoroid shots) were made on sequence 1, and 9 test firings on sequence 3. The energy required to break wires within the cable (breakpoint) was determined to lie between 8.64 and 11.0 joules. Since there were no shorts in this type of cable, no leakage tests were performed. An evaluation test was made on a few cables. It was found that a maximum of 40 percent of the strands in one wire were broken, but sufficient data were not accumulated to establish this as an average figure. Figure 12 depicts typical damage to cable type 1.

Type 2 is a single-shielded wire cable. A total of 12 direct test firings, sequences 7 and 9, were made on this cable. The test results indicate that the energy required to short conductors to shields lies between 0.164 and 0.210 joule. The leakage test revealed that for this type of cable, an average current of approximately 4.66 amperes is required to open a short between the shield and a conductor. Test number 38, however, had the following results. The test cable (number 10) experienced many shorts, two of which required 9 amperes of current per short to be burned open. One short when opened became a

Figure 12. Typical damage to cable type 1.

high-resistance short of 82.9 MΩ. It would be highly improbable that a short of this type, in normal Skylab operation, would ever be burned open. This was, however, the only case where this problem arose. The evaluation test revealed that a minimum amount of damage was done to the wire. An average of 20 percent of the strands in one wire were broken. Refer to Figure 13 for typical damage to cable type 2. The breakpoint of this cable was not determined.

Type 3 is an overall shielded cable. Six test firings, sequences 11 and 12, were made on this cable. The energy required to short conductors to shields was found to lie between 2.03 and 2.62 joules. The leakage test results indicated that an average of 9 amperes of current was required to burn off a short to the shield. There were many cases, however, where the shorts were never opened, even when this amount of current remained on the wire for a period of 1 to 5 minutes. The evaluation test revealed that little damage was done to the wire. Only in one case was there excessive damage where 60 percent of the strands in one wire were broken. Figure 14 depicts typical damage to cable type 3.

Type 5 is coaxial cable. A total of 10 test firings were made, and the breakpoint was determined to be between 10.2 and 11.4 joules of energy, very similar to that found for unshielded wire cable. The cables were subjected to an RF test before and after the test shots; no electrical characteristics of the cable changed appreciably, and the only failure observed was open wire. See Figure 15 for typical damage to cable type 5.

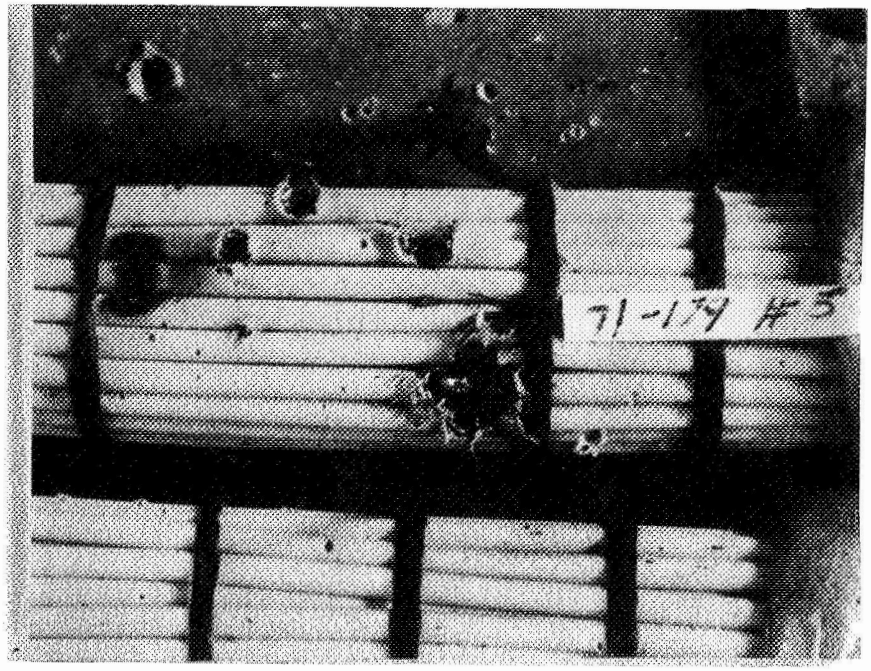

Figure 13. Typical damage to cable type 2.

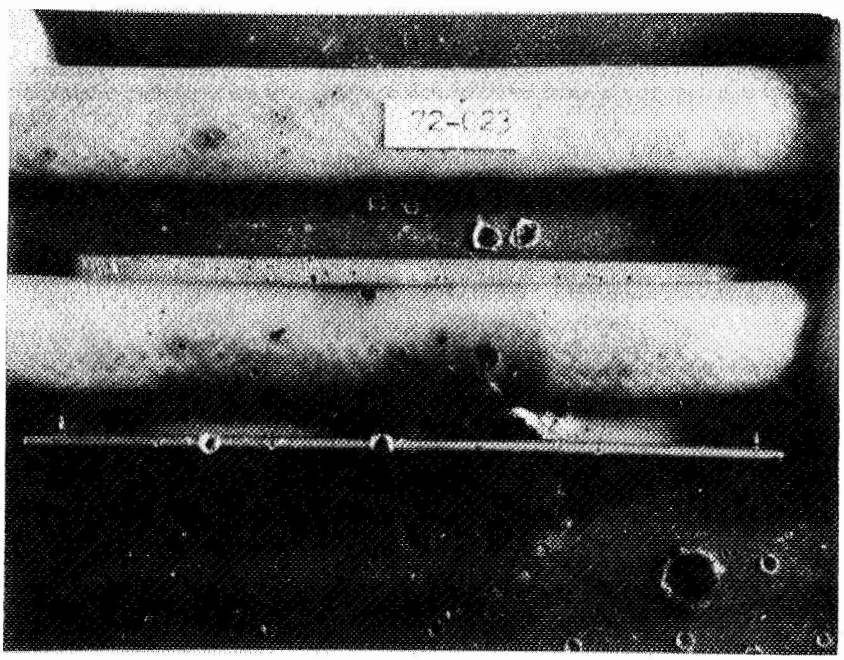

Figure 14. Typical damage to cable type 3.

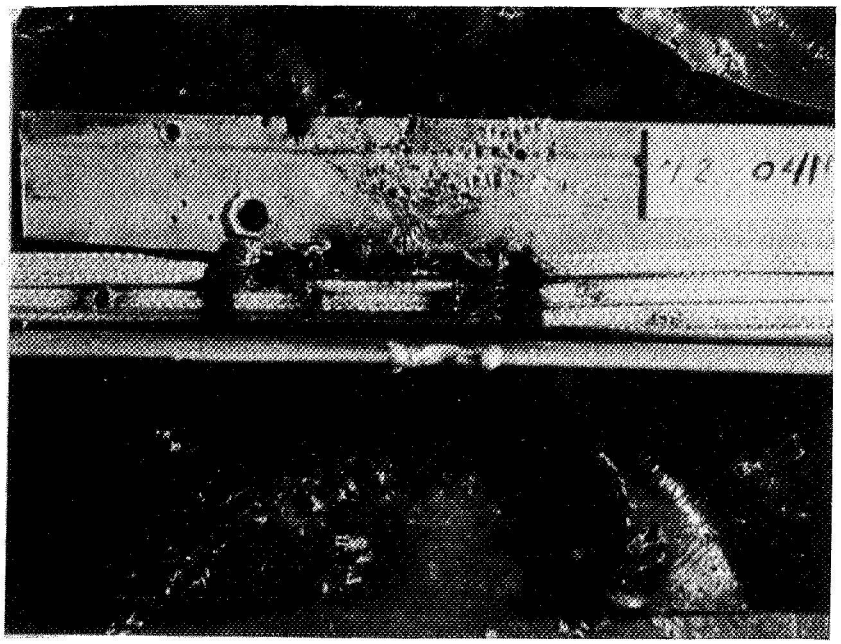

Figure 15. Typical damage to coaxial cable type 5.

Type 7 is flat cable. A total of 12 test firings were made, and the breakpoint was found to lie between 2.68 and 5.68 joules of energy. However, the breakpoint was also found to be dependent on the size and, to some degree, the location of the hit. If the micrometeoroid mass was approximately 1×10^{-5} g, the conductor did not open. The conductor was penetrated but remained undamaged to the extent that the current- or signal-carrying capability of the wire was not impaired. If, however, the micrometeoroid mass was approximately 1×10^{-4} g and hit the conductor dead center or a slight margin from the center, the conductor opened. Figure 16 depicts typical damage to cable type 7.

The results described indicate that the shielded wire cables are significantly more sensitive to micrometeoroid bombardment than are unshielded wires. However, all cables can withstand a higher degree of damage than previously anticipated.

It was found that for the unshielded wire cable, the common mode of failure was an open conductor resulting in the loss of that conductor within a cable. But mission-critical circuits are redundant; consequently, this is not catastrophic. However, for the shielded wire cables, the most common failure was one or more conductors shorting to the shield. For single-shielded wire cable, 4.66 amperes of current were required to open a short, and for overall shielded wire cable, 9 amperes of current were required. Since the shielded cables are almost always signal cables, the possibility of the short opening is remote. This could result in the mixing up of signals, possible grounding of circuitry, load changes, etc.

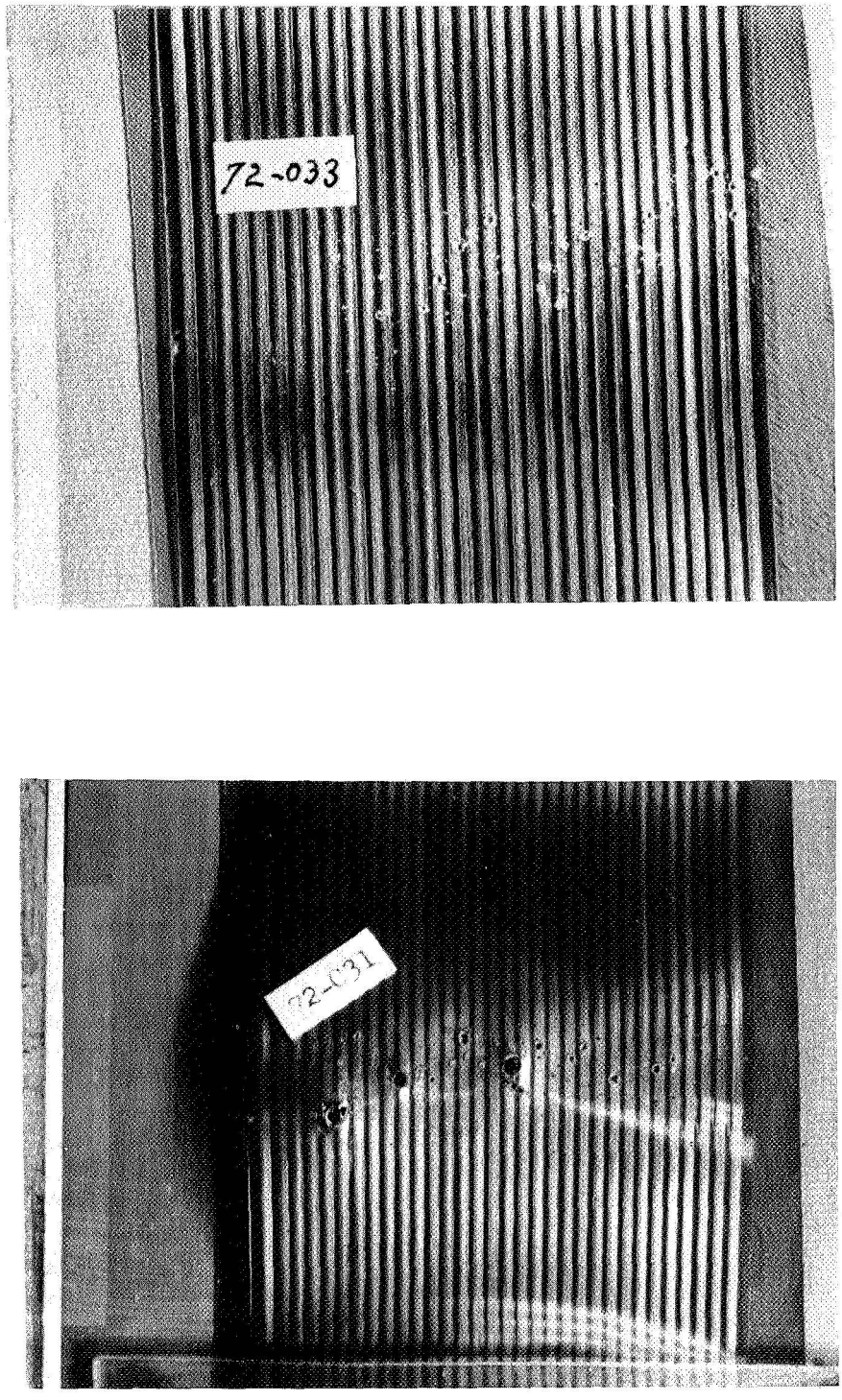

DAMAGE FROM 2.76 × 10^{-4} g BEADS

Figure 16. Typical damage to flat cable type 7.

Protection of all Skylab exposed cabling is extremely difficult; therefore, only mission-critical cables should be considered. Shielded cables are not generally mission-critical cables, and this problem is not as grave as previously determined.

A worst-case analysis on exposed Skylab cabling is currently in progress, and only mission-critical cables are being considered, as exposed to the micrometeoroid environment. The results of the analysis will be completed by April 30, 1972, and made available from ASTN-ES.

III. DATA

For this investigation, 68 test firings and 12 calibration firings were made, and 10 different sequences were tested.

The tests are separated into two main categories: direct impact of projectiles on the cable, and indirect impacts with the cable behind a micrometeoroid bumper. The bumper was 0.064-cm (25-mil) thick aluminum, spaced 12.7 cm (5 in.) above the cable to simulate the OWS bumper.

Each category was broken down as follows:

a. Current-carrying cables and zero-current (no voltage) cables – The zero-current cables had no electrical connections during the firings, but were checked after the firings for shorts and opens.

A number of the firings were made against two cables simultaneously, one a current-carrying cable and the other a zero-current cable. The number of firings was reduced by this technique; however, it was found that one cable received less hits than the other cable (see test 43 of sequence 3 for comparison). Refer to Section IV for explanation.

b. Cable types – These cable types were as follows: (1) unshielded wire laced into a cable (type 1), (2) individually shielded wire laced into a cable (type 2), (3) unshielded laced wire covered with an overall shield and a protective heat shrink tubing (type 3), (4) coaxial cable RG-179 (type 5), and (5) 32-conductor flat cable (type 7).

In the interpretation of test data, several uncontrollable variables must be considered: (1) number of pellets hitting the cable, (2) some pellets hitting the cable head-on and some hitting on the side of the cable, (3) more than one pellet hitting in approximately the same area, and (4) the arrangement of 30- and 60-volt coil wires in the cables.

Actual micrometeoroids are expected to be singular hits rather than multiple hits. The test cables were designed to have 30- and 60-volt coil wires adjacent to each other; however, the possibility existed of having similar wires adjacent.

These data are not exactly comparable to data which might be obtained from testing with actual micrometeoroids. The tests were performed with glass beads, "Lexan" plastic cylinders, and syntactic foam cylinders with densities of 2.5, 1.25, and 0.7 g/cm^3, respectively, and at velocities between 4 and 8 km/s. The majority of micrometeoroids have approximate densities of 0.5 g/cm^3 and velocities of about 20 km/s.

A. Description

The data from these firings consist of test data sheets, pictures of the cables after the firings, pictures of the oscilloscope traces, fact test data sheets, and leakage test data. These data are available for review but are not attached.

The test data sheets contain information identifying the firing and the cables used, plus resistance and voltage measurements made before and after the firings. These measurements assure that the cable was correctly wired before the firing and indicate broken wires and permanent shorts between coils.

Pictures taken of the cables after the firings contain information on the location of hits, side or head-on, and the amount of damage to the cable.

The oscilloscope used was a dual trace type which presents the 30- and 60-volt coil traces together on a picture and facilitates comparisons.

Fact test printouts indicate all shorts and opens in the cable.

Leakage test data sheets indicate the voltage and current required to burn open the short and its measured resistance.

Appendix B discusses an interpretation of the oscilloscope pictures.

Physical damage to cables may be misleading since a shielded cable hit by small pellets appears to be perfect except for a few minor pinholes. However, four shorts were found between shield and wire when tested.

The fact tests of shielded wire sometimes indicate shorts between conductors as well as shorts between shield and wire. Indications of conductor shorts were found to be due to the electrical path through the shield. The fact tests of shielded wire cable in some cases showed shorts which disappeared between the fact and leakage tests. Two possible explanations are that the short may have been in the megohm region or that the short disappeared because of jarring during transportation between the two testers which were in different buildings. Some procedural changes were made during the tests as better methods were discovered. Firings were made at single cables during sequences 1 and 3, except for tests 23 and 43. Most of the later tests were made with two cables at one time. Cables were loosely fastened with tape to the backup plate during early firings, but were clamped rigidly to the plate in later firings. A second oscilloscope was added for observing the 30-volt coil for a longer period of time. This scope was later used to observe the voltage across a shunt which was placed in the shield to ground lead.

B. Conclusion

Testing is needed to more accurately evaluate bumper debris damage to shielded wire cables. Some additional tests of overall shielded cables in the lower pellet energy area will permit better identification of the breakpoint.

A summary of test data obtained is given in Tables 1, 2, and 3.

IV. EXPERIMENTAL PROCEDURE

A. Test Parameters

1. Accelerators. The accelerator used for this test series was a two-stage, 0.3175-cm (1/8-in.) light gas gun. Hydrogen was used to accelerate the projectile. The highest velocity obtained to date with this accelerator is 9.80 km/s.

2. Range. The range has a free path approximately 6.0 m long. Three photomultiplier tubes and two photo FET transducers are stationed along this free flight path. The output signals of these five devices establish a time of flight from which the velocities are calculated.

The tests were conducted with a range pressure of 10 mm of mercury, created by introducing argon into the range after the evacuation. This environment was necessary to allow the photomultiplier tubes and photo FET transducers to establish time of flight.

3. Projectiles. The projectiles used for this test series were cylinders and glass spheres. The material used to make the cylinder was "Lexan," which has a density of 1.25 g/cm^3, and syntactic foam which has a density of 0.7 g/cm^3. The glass spheres have a density of 2.5 g/cm^3. The cylinders were used for the indirect tests.

The method of launching the glass spheres was similar to a shotgun in that the distribution of the spheres was concentrated toward the center. The "wad" used was a "Lexan" cylinder; therefore, placing the cables in a position where the concentration of spheres would hit was extremely difficult. A compromise was made to place one cable (inner cable) closest to the periphery of the "wad" damage area and the other cable (outer cable) on the outside of this inner cable.

4. Targets. The targets are described in Section II and in Appendix A.

B. Procedure

Several tests were conducted for calibration to determine whether the argon gas, used for obtaining the desired velocity, or the acceleration gases would have any measurable effects; it was found that they had no effect.

TABLE 1. COMBINED CABLE TEST RESULTS, DIRECT PELLET IMPACT

Unshielded (Type 1)					Shielded (Type 2)					Overall Shield (Type 3)				
Test No.	Seq. 1 Result	Energy (J)	Seq. 3 Result	Pellet Size (cm)	Test No.	Seq. 7 Result	Energy (J)	Seq. 9 Result	Pellet Size (cm)	Test No.	Seq. 11 Result	Energy (J)	Seq. 12 Result	Pellet Size (cm)
3	Pulse	5.8	–	0.06	44	OK	0.15	–	0.018	54	–	0.17	OK	0.018
64	–	8.6	OK	0.08	41	OK	0.16	No hits	0.018	58	Pulse	2	OK	0.042
23	Open	11	Open	0.1	54	–	0.17	OK	0.018	61	No hits	2.4	OK	0.05
65	–	12.6	OK	0.08	40	Wad Burn	0.17	Short	0.021	63	OK	2.6	Short	0.05
14 (67)	Pulse	13.3	Open	0.07 (0.1)	59	–	0.19	OK	0.018	66	Open	2.8	OK	0.05
43	–	14.4	Open	0.1	45	Short	0.21	–	0.021	60	OK	4.6	Short	0.05
43	–	14.4	OK	0.1	39	Short	0.59	Short	0.03	57	Open	5.9	Short	0.06
16	Open	16.8	–	0.08	38	Wad	0.62	Short	0.03					
15	Pulse	17	–	0.08	42	Short	0.7	Wad	0.03					
20	OK	18.3	–	0.1	37	Short	2.1	Short	0.042					
9	Open	19.1	–	0.1	35	Short	4.4	Short	0.06					
52	–	22.9	Open	0.1	36	Short	4.6	No hits	0.06					
					34	Open	15.2	–	0.1					

Cable Locations

Seq. 1 & 3 – Single cable tests except for test 23 and 43. The second listing for test 43 was the outside cable.

Seq. 7 & 9 – Seq. 9 cables were the outer cables.

Seq. 11 & 12 – Seq. 11 cables were the outer cables except in test 66 when the Seq. 11 cable was the inside cable.

Seq. 2 & 4 – Unknown

Seq. 8 & 10 – Seq. 10 cables were the outer cables.

Code

Pulse – A pulse on the oscilloscope.

Open – One or more wires broken

OK – No pulse, short or open

Short – Short between wires or between shield and wires.

No hits – Cable not hit by projectile

Wad – The wad or its debris hit cable

Strip – Insulation removed from one or more wires

– No test made in this sequence.

TABLE 2. COMBINED CABLE TEST RESULTS, MICROMETEOROID BUMPER

Unshielded (Type 1)						Shielded (Type 2)					
Test No.	Seq. 2 Result	Energy (J)	Seq. 4 Result	Pellet Size (cm)	Velocity (km/s)	Test No.	Seq. 8 Result	Energy (J)	Seq. 10 Result	Pellet Size (cm)	Velocity (km/s)
24	OK	11	OK	0.1	4.1	56	OK	630	OK	0.33 X 0.17	8.5
25	OK	12.4	OK	0.1	4.6	55	Open	678	Short	0.33 X 0.33	6.4
26	OK	747	OK	0.33 X 0.25	7.7	62	Short	716	Short	0.33 X 0.25	7.5
46	–	845	OK	0.33 X 0.25	8.2	47	Short	760	OK	0.33 X 0.25	7.8
29	Wad	1056	Wad	0.64 X 0.64	4.0						
31	Pulse	1164	–	0.64 X 0.64	4.2						
49	–	1172	OK	0.48 X 0.25	7.0						
30	OK	1385	OK	0.64 X 0.64	4.7						
48	–	1700	OK	0.48 X 0.48	5.8						
27	Pulse	2353	OK	0.48 X 0.48	6.9						
28	Open	3012	Short	0.64 X 0.64	5.0						
32	Pulse	3241	–	0.64 X 0.64	7.2						
50	–	3540	Strip	0.66 X 0.48	6.3						

TABLE 3. COMBINED CABLE TEST RESULTS, FLAT CABLE AND COAXIAL CABLE

Flat Cable (Type 7)						Coaxial Cable Bundle (Type 5)				
Test No.	Result	Energy (J)	Velocity (km/s)	Pellet Size (cm)	Wire Removed by Center Hits (%)	Test No.	Result	Energy (J)	Velocity (km/s)	Pellet Size (cm)
71	OK	0.54	5.62	0.0297	40	81	OK	5.7	6.43	0.0595
72	OK	1.45	7.06	0.0354	90	90	OK	9.4	6.30	0.0707
70	OK	2.49	7.17	0.042	90	80	OK	10.2	6.67	0.0707
73	OK	2.68	5.72	0.05	No center hits	78	OK	10.2	5.14	0.0841
69	Open	5.68	6.42	0.0595	100	79	Open	11.4	7.04	0.0707
88	OK	6.09	5.13	0.0707	90+	85	Open	11.9	4.26	0.1
83	OK	7.59	5.66	0.0707	90+	86	Open	16.4	5.01	0.1
84	Open	12.5	7.29	0.0707	100					

Resistance and voltage measurements were recorded before and after each shot as described in the test procedure. An oscilloscope was used to monitor the voltage on each circuit during the impact event. The scope was triggered from the pulse of the third photomultiplier tube so that it would monitor the circuit approximately 50 to 100 μs before the impact. The cables were then removed from the range and subjected to the tests as described in Section III, Data.

A photograph of the complete test setup is shown in Figure 17.

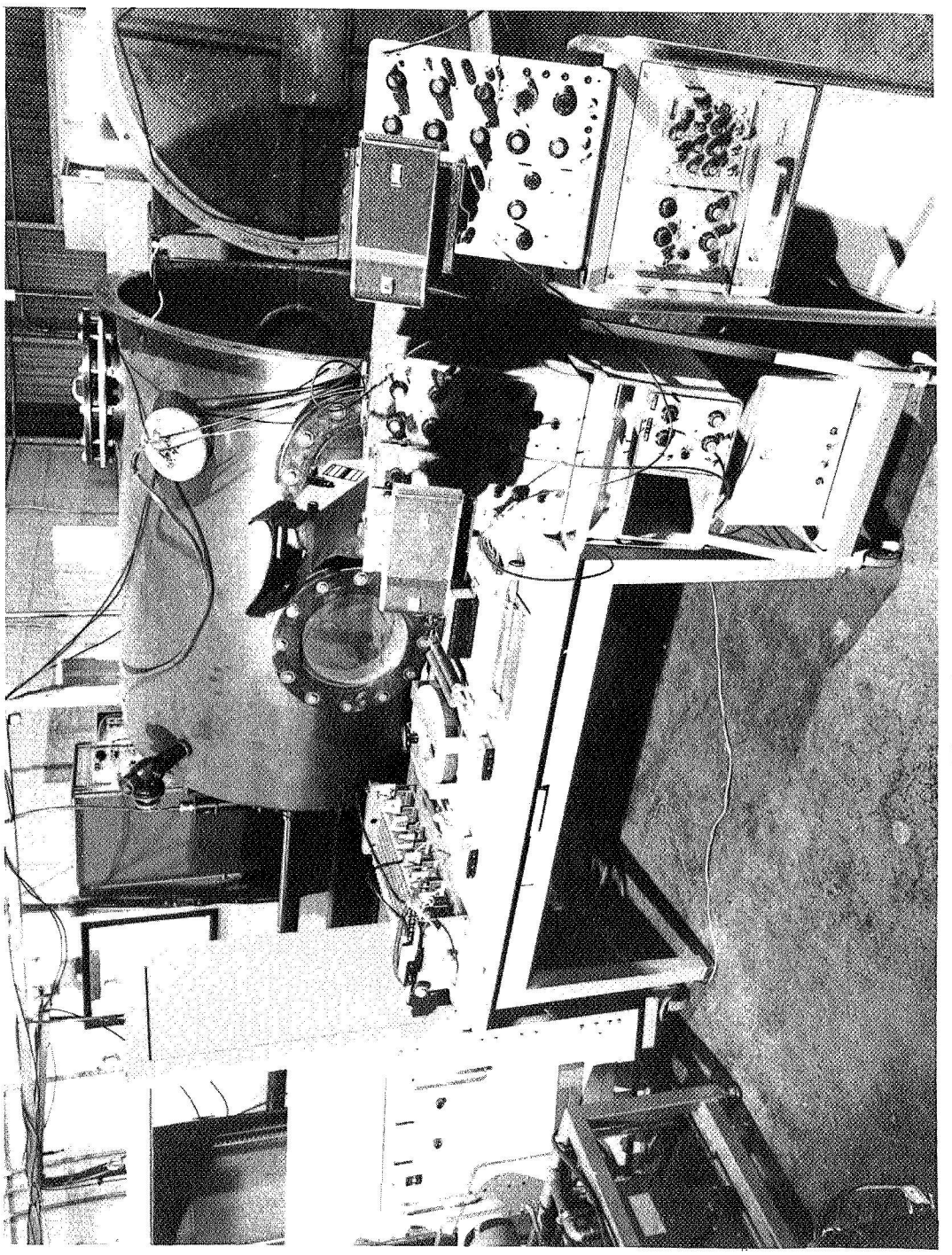

Figure 17. Test setup.

APPENDIX A. MICROMETEOROID TEST PROCEDURE

1. Purpose

This document establishes the procedure for micrometeoroid testing of typical exposed Skylab cabling and harness assemblies.

2. Objective

The objective is to determine the energy levels of micrometeoroids that may cause cable failures during the Skylab Mission. Because of the lack of test facilities with a capability to actually simulate space conditions (lightweight micrometeoroids at average speeds of 20 km/s), data must be obtained at less stringent conditions, and predictions or extrapolations must be made.

3. Test Specimen Requirements

a. General Requirements. The test specimens will be representative Skylab cable types. The following general notes will apply:

1. Wire Specifications – All unshielded wire will conform to MSFC-SPEC-40M39513/5. All shielded wire will conform to MSFC-SPEC-40M39526A/5.

2. Twisted Wires – Where wires are to be twisted, there will be a minimum of 2.44 twists (transpositions) per meter (8 twists per foot), or a maximum lay of 7.62 cm (3 in.).

3. Lacing – Wires will lay as straight as practical in the cable harness and lacing will conform to Style A of MSFC-STD-40M39582.

4. Shields – Shields will be terminated per Standard MSFC-STD-40M39582, Class 5. All shields will be insulated from each other and the vehicle skin. Heat reactive tubing per MSFC-SPEC-276B, Type II, Class 1A may be used if necessary.

5. Contacts – Contacts will be installed and crimped per MSC/MSFC JD-001, dated February 16, 1966.

6. Cleaning – Cables will be wiped clean by using a lint-free cloth or sponge and isopropyl alcohol as required. After cleaning, cables will be blown dry with clean, dry air. Cables will not be submerged in alcohol.

b. Specific Requirements. Five types of cables will be considered as test specimens. Priority will be given to the testing of cable types 1 and 2. Other cable types will be tested as time and scheduling permits:

1. Cable Type 1 – Unshielded wire type V6N20N, wire electrical insulation Type V20 AWG 40M39513A/5. Connector and overall configuration will be as indicated in Figure A-2.

2. Cable Type 2 – Shielded wire type V6N20N1NB, wire electrical insulation type V20 AWG 40M39526A/5. Connector and overall configuration will be as indicated in Figure A-2.

3. Cable Type 3 – Wire type V6N20N, wire electrical insulation type V20 AWG 40M39513A/5 with overall shield. Connector and overall configuration will be as indicated in Figure A-3.

4. Cable Type 4 – Unshielded wire type V6N16N wire electrical insulation Type V16 AWG 40M39513A/5. Connector and overall configuration will be as indicated in Figure A-4.

5. Cable Type 5 – Coaxial cable type RG 179B/U per MIL-C-17D. Connector and overall configuration will be as indicated in Figure A-5.

6. Cable Type 6 – Unshielded wire type V6N12N wire electrical insulation. Type V12 AWG 40M39513A/5. Connector and overall configuration will be as indicated in Figure A-6.

7. Cable Type 7 – 32-conductor flat cable.

4. Test Preparation and Descriptions

a. Test Flow Plan. Priority will be given to testing cable types 1 and 2. Other cable types will be tested as time and scheduling permits. The test flow plan is given in Table A-1. The number of test specimens selected is based on making predictions as indicated in Paragraph 2 above. If the decision is made to extrapolate, many more test specimens and test firings (see Paragraph e below) may be required.

b. Test Specimen Identification. Prior to testing each test specimen will be identified with a tag that will accompany the specimen throughout testing. The tag will properly identify the test specimen and will summarize fact test results (see Paragraph f. below). If a test specimen is used (hit by micrometeoroid firing) more than once, the specimen damage will be identified according to test firing.

c. Mounting Considerations. Each test specimen will be rigidly mounted on a test fixture prior to testing. The specimen will retain that configuration throughout the test sequence. If the after impact fact test indicates no failures, the test specimen may be removed from the plate and used in another test firing. A surface that has not been fired upon will be used for the second firing.

d. Test Data Sheets. An example test data sheet is given later in this appendix. All entries that are applicable to the test will be made during testing. A test data sheet will be required for each test specimen in each test firing.

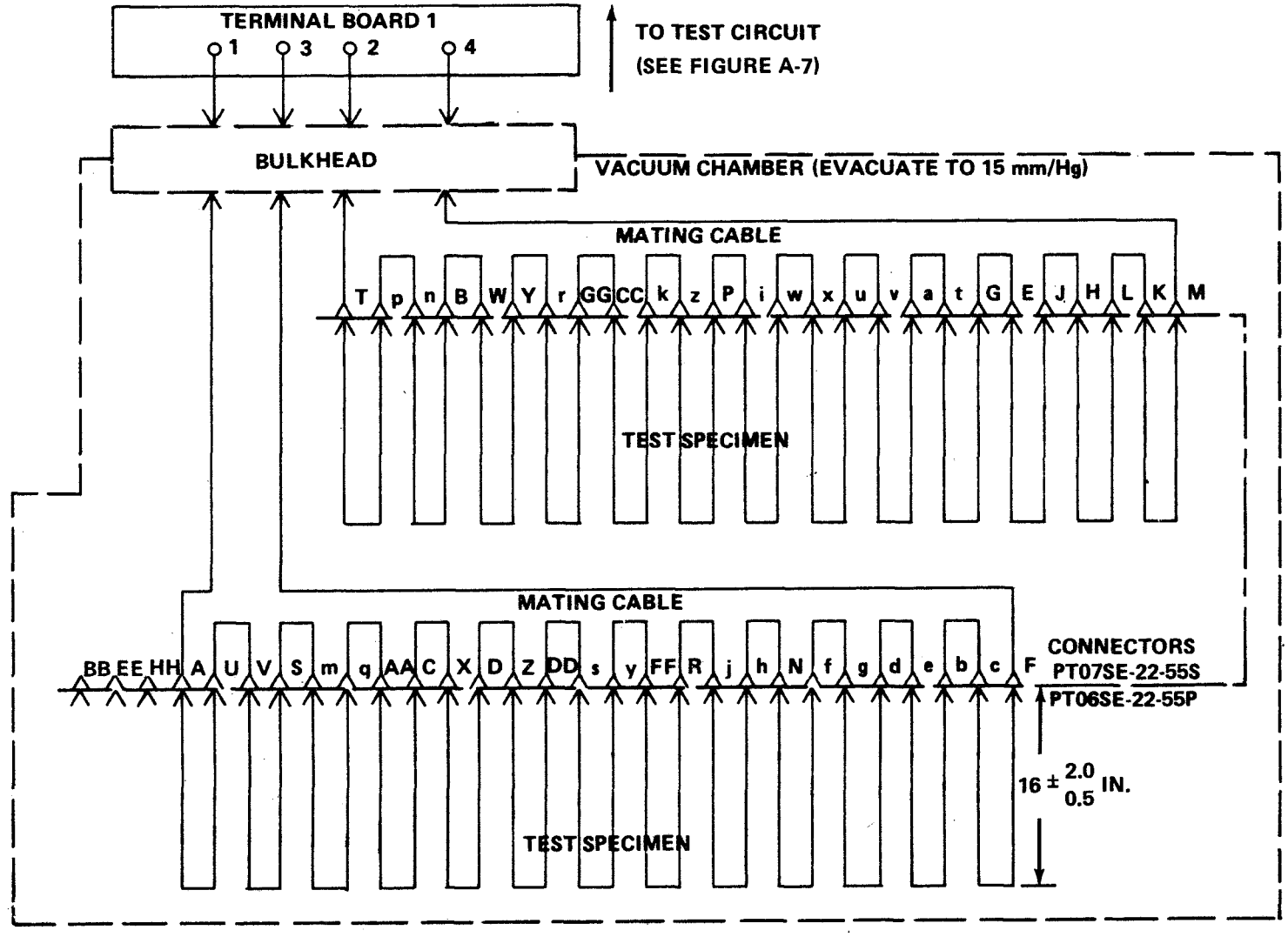

Figure A-1. Cable type 1 in vacuum chamber.

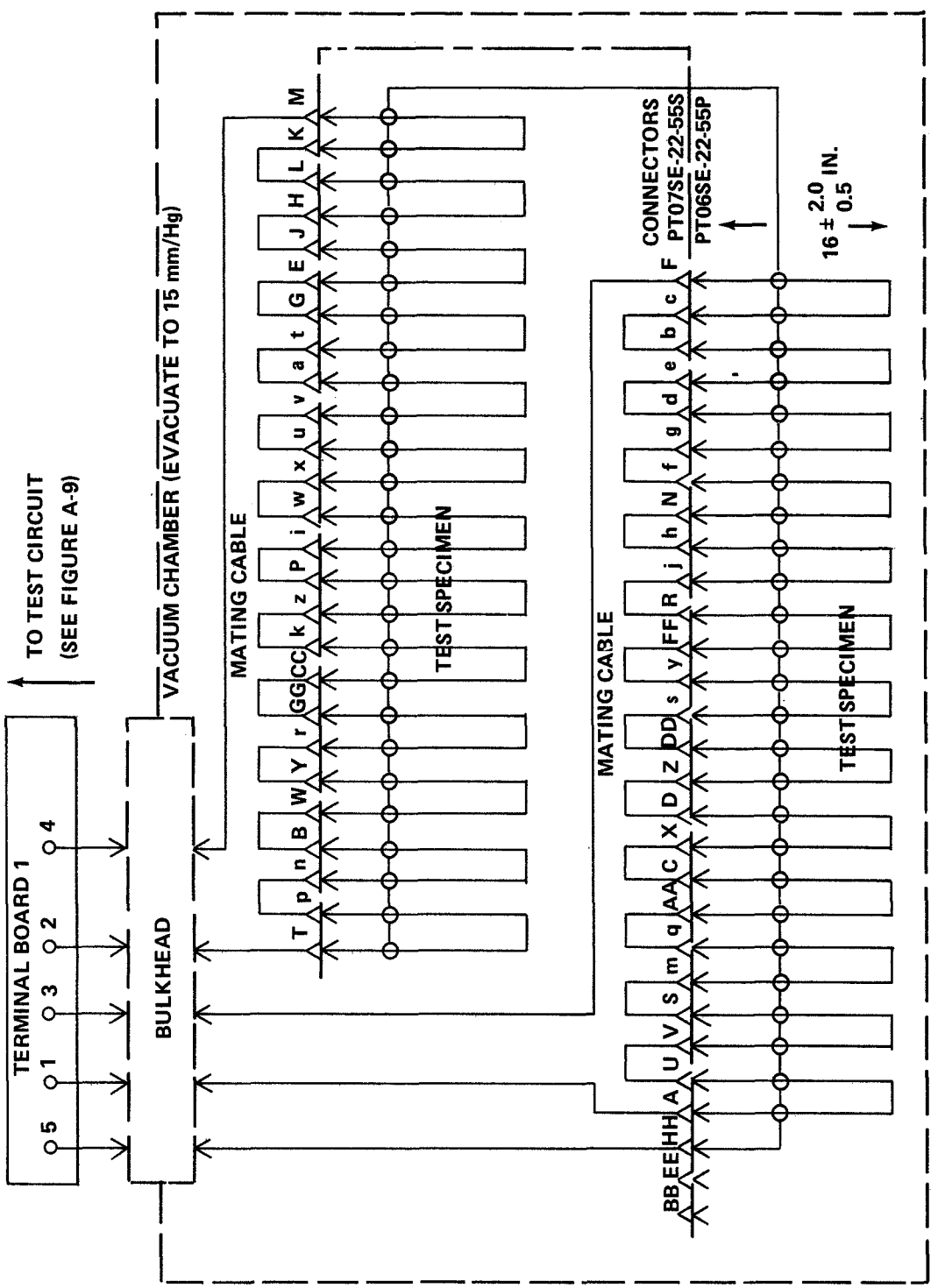

Figure A-2. Cable type 2 in vacuum chamber.

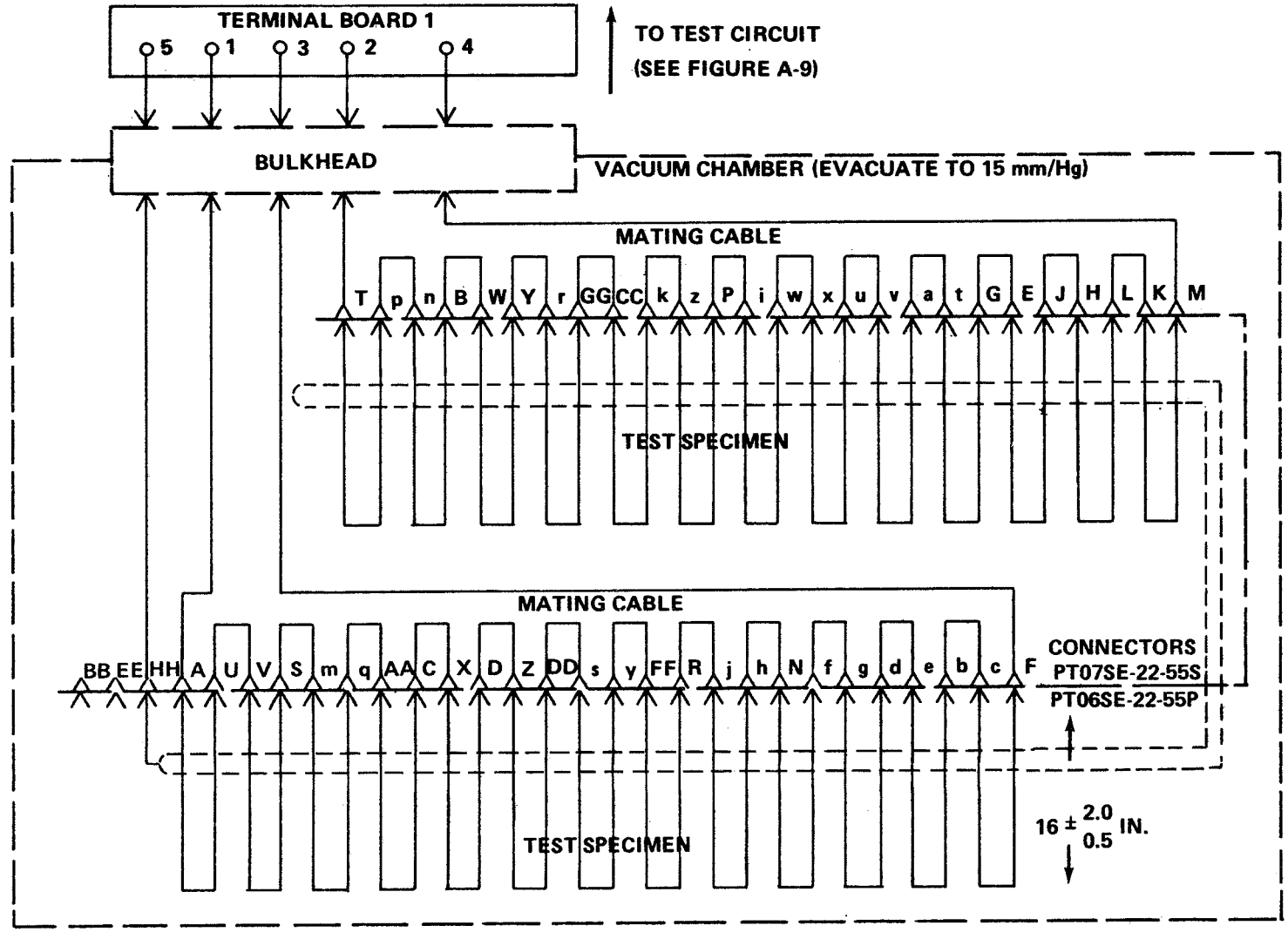

Figure A-3. Cable type 3 in vacuum chamber.

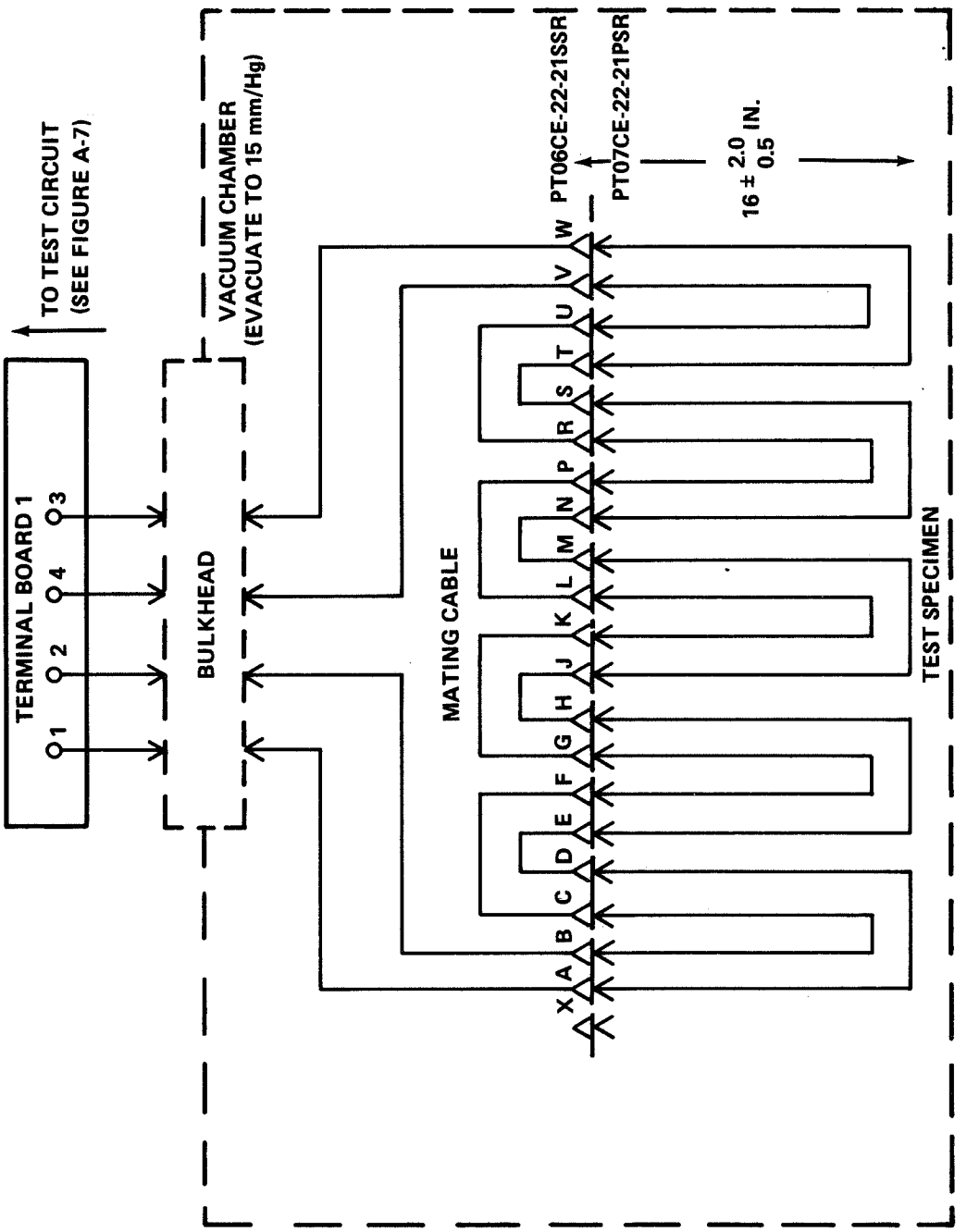

Figure A-4. Cable type 4 in vacuum chamber.

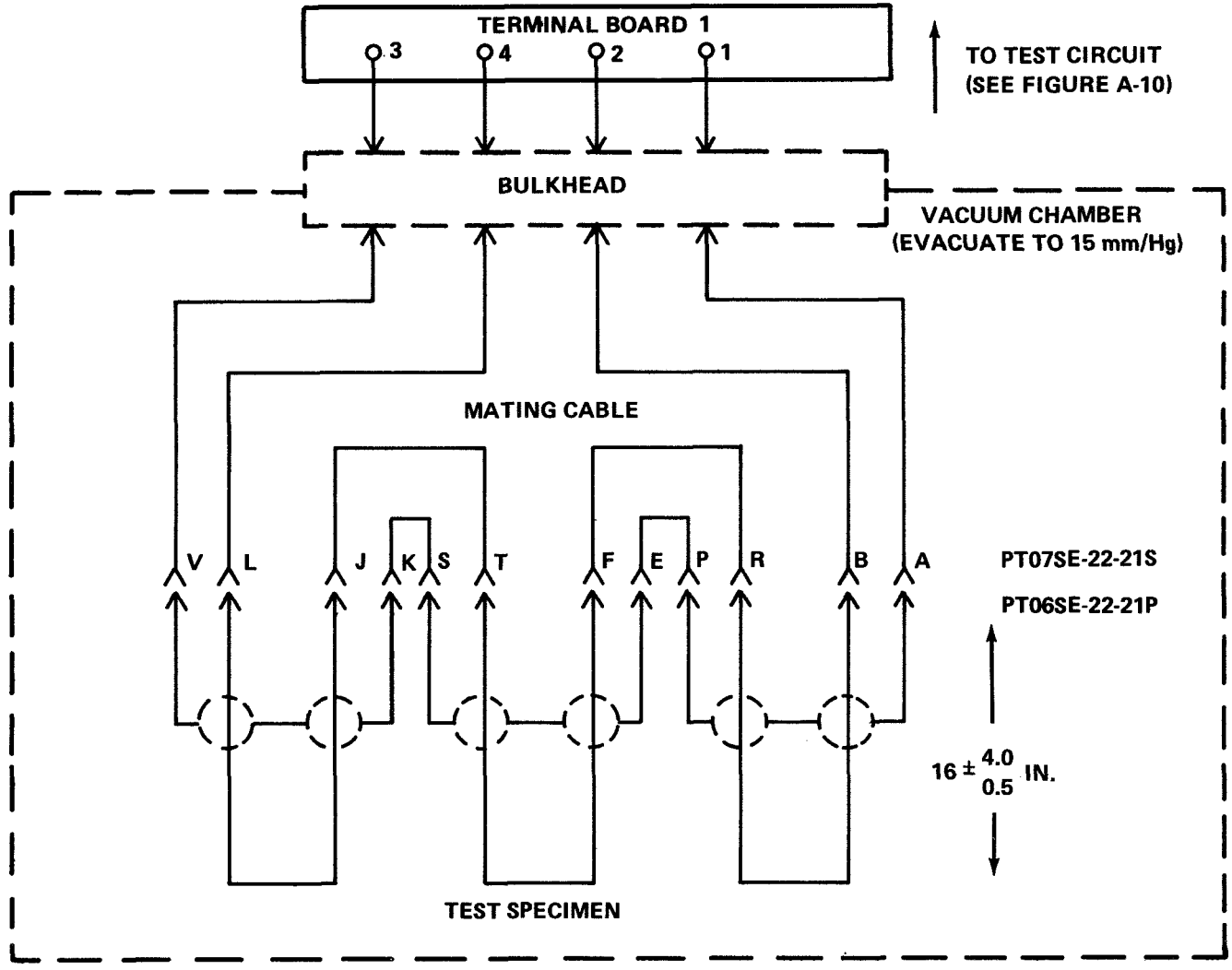

Figure A-5. Cable type 5 in vacuum chamber.

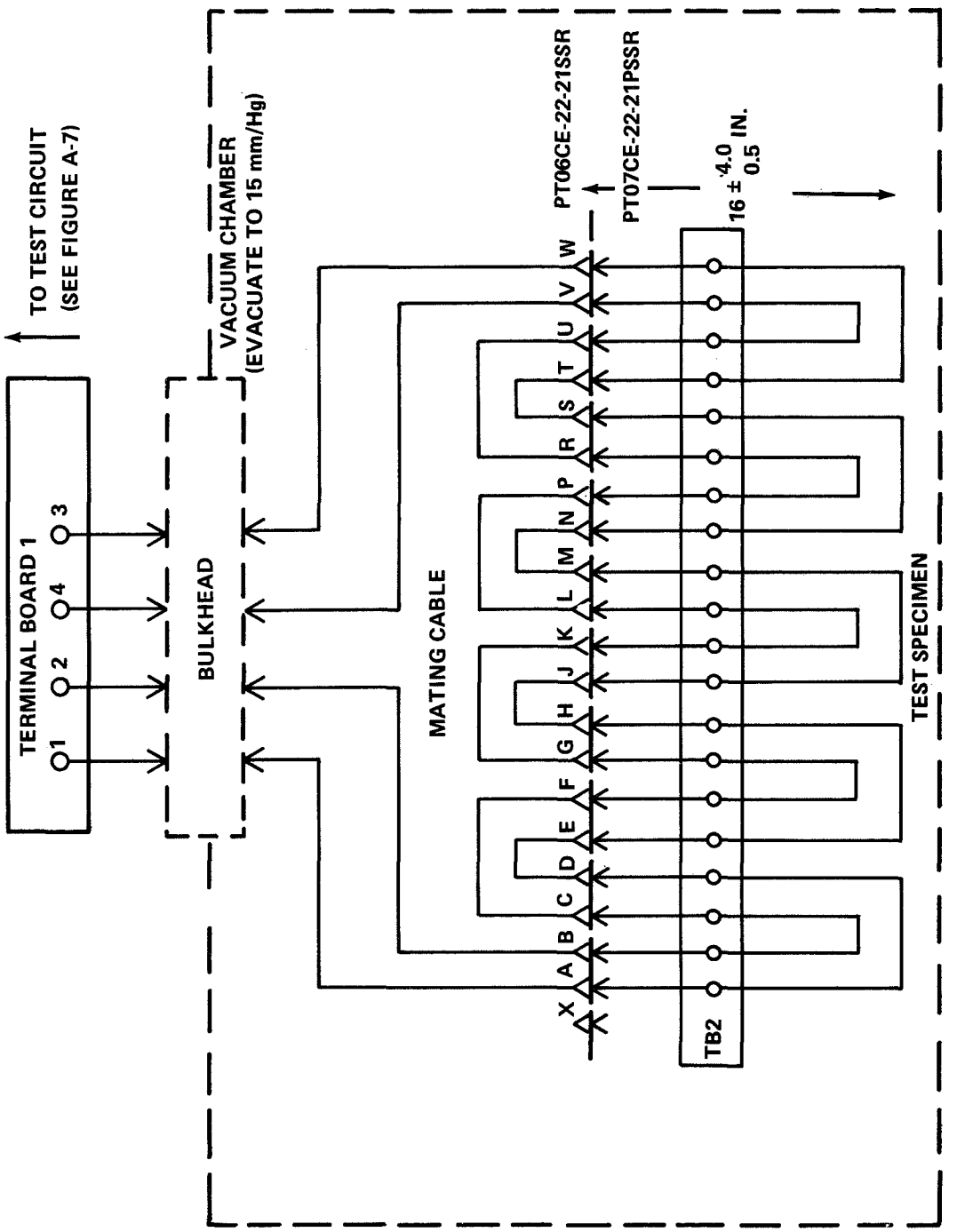

Figure A-6. Cable type 6 in vacuum chamber.

TABLE A-1. SKYLAB CABLES MICROMETEOROID TEST FLOW PLAN

Test Sequence	Completed or Uncompleted	Cable Type	Monitor Circuit	Micrometeoroid Impact	Probable Number of Test Specimens Required
1	Completed	1	Fig. A-7	Direct	5
2	Completed	1	Fig. A-7	Indirect	5
3	Completed	1	None	Direct	5
4	Completed	1	None	Indirect	5
5		1	Fig. A-8	Direct	5
6		1	Fig. A-8	Indirect	5
7	Completed	2	Fig. A-9	Direct	5
8	Completed	2	Fig. A-9	Indirect	5
9	Completed	2	None	Direct	5
10	Completed	2	None	Indirect	5
11	Completed	3	Fig. A-9	Direct	5
12	Completed	3	None	Direct	5
13		4	Fig. A-7	Direct	5
14		4	None	Direct	5
15		5	Fig. A-10	Direct	5
16	Completed	5	None	Direct	5
17		6	Fig. A-7	Direct	5
18		6	None	Direct	5
19	Completed	7	None	Direct	1

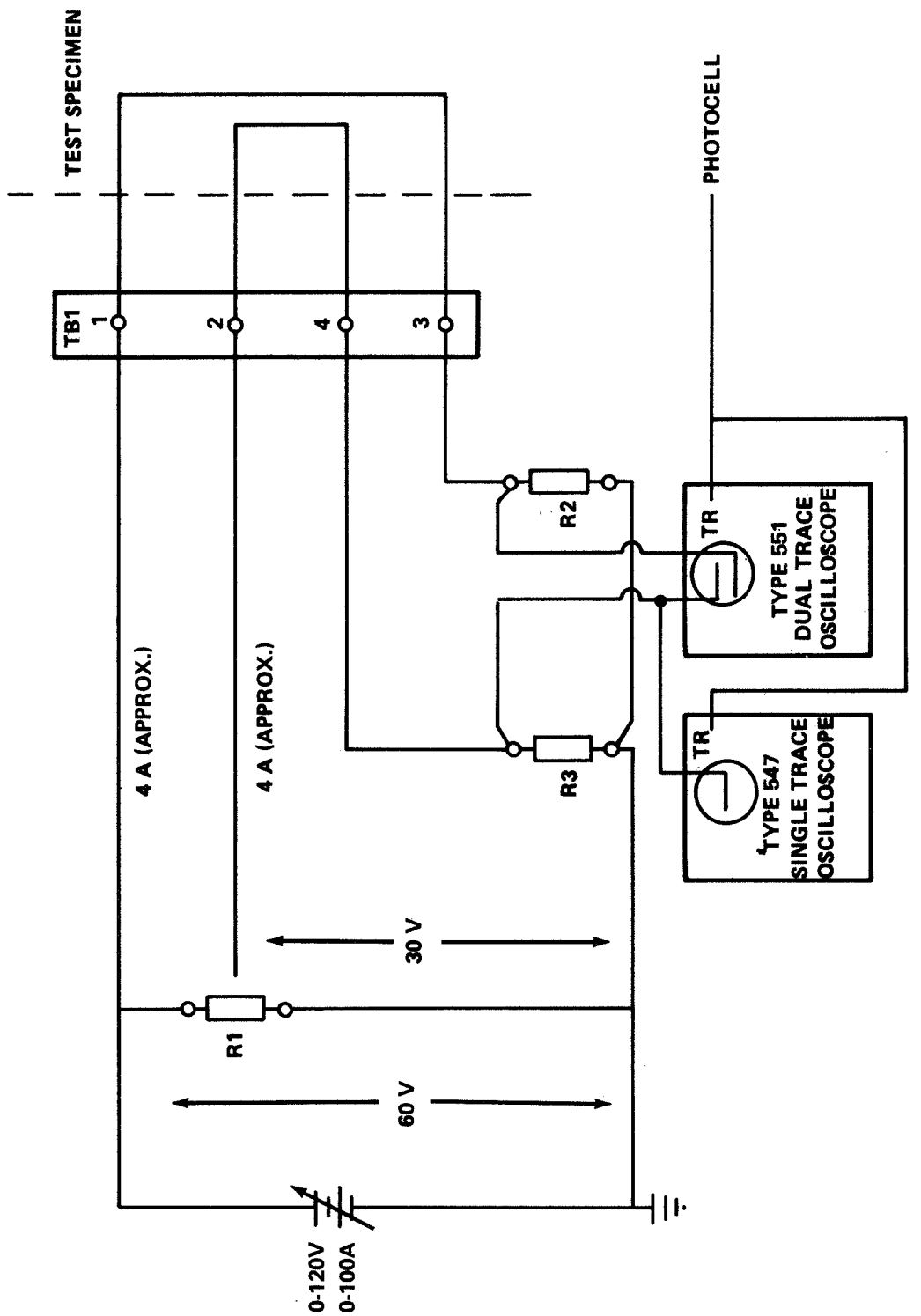

Figure A-7. Test monitor circuit for cable types 1, 4, and 6.

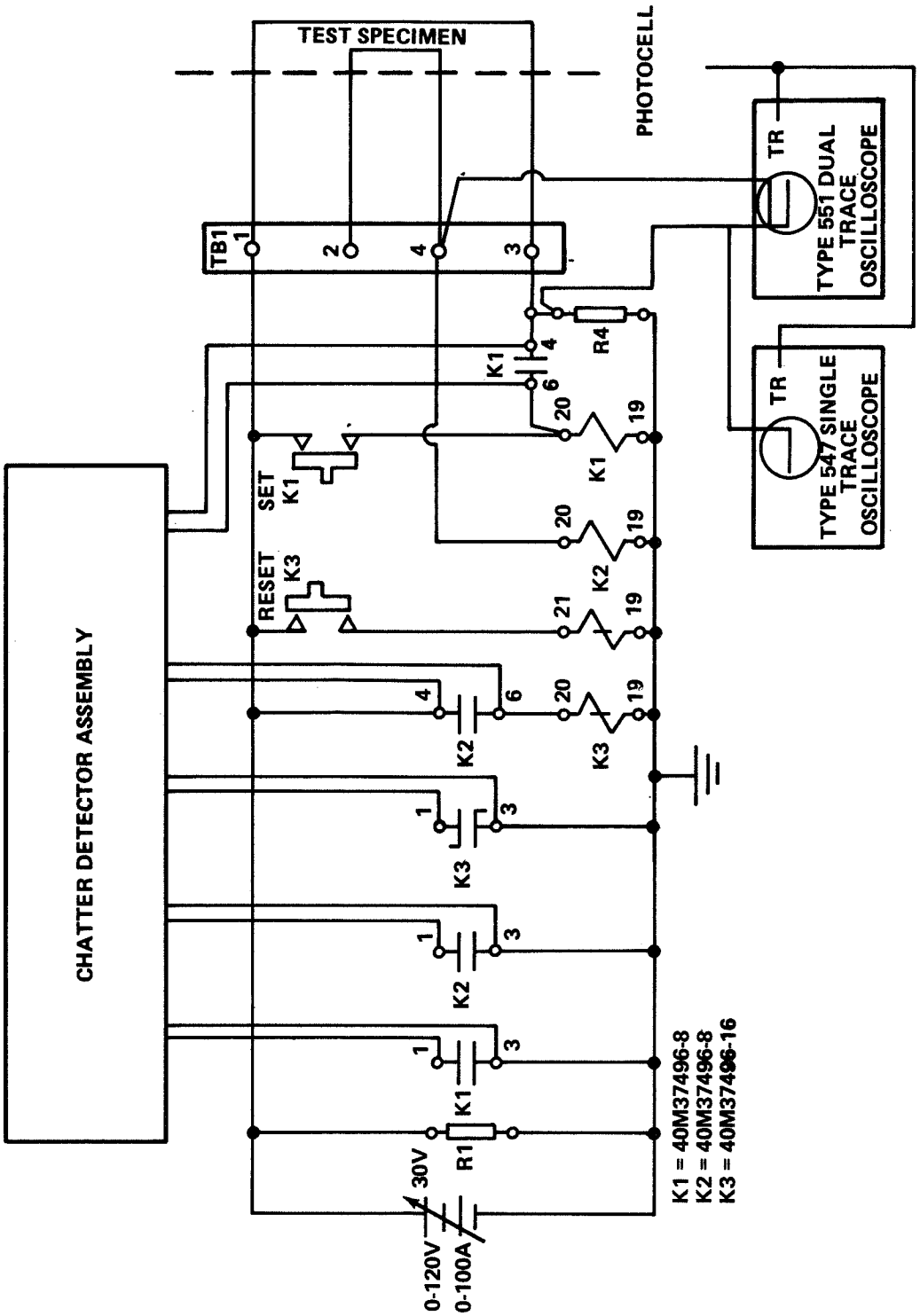

Figure A-8. Test monitor circuit for typical type 1 cables and a relay circuit.

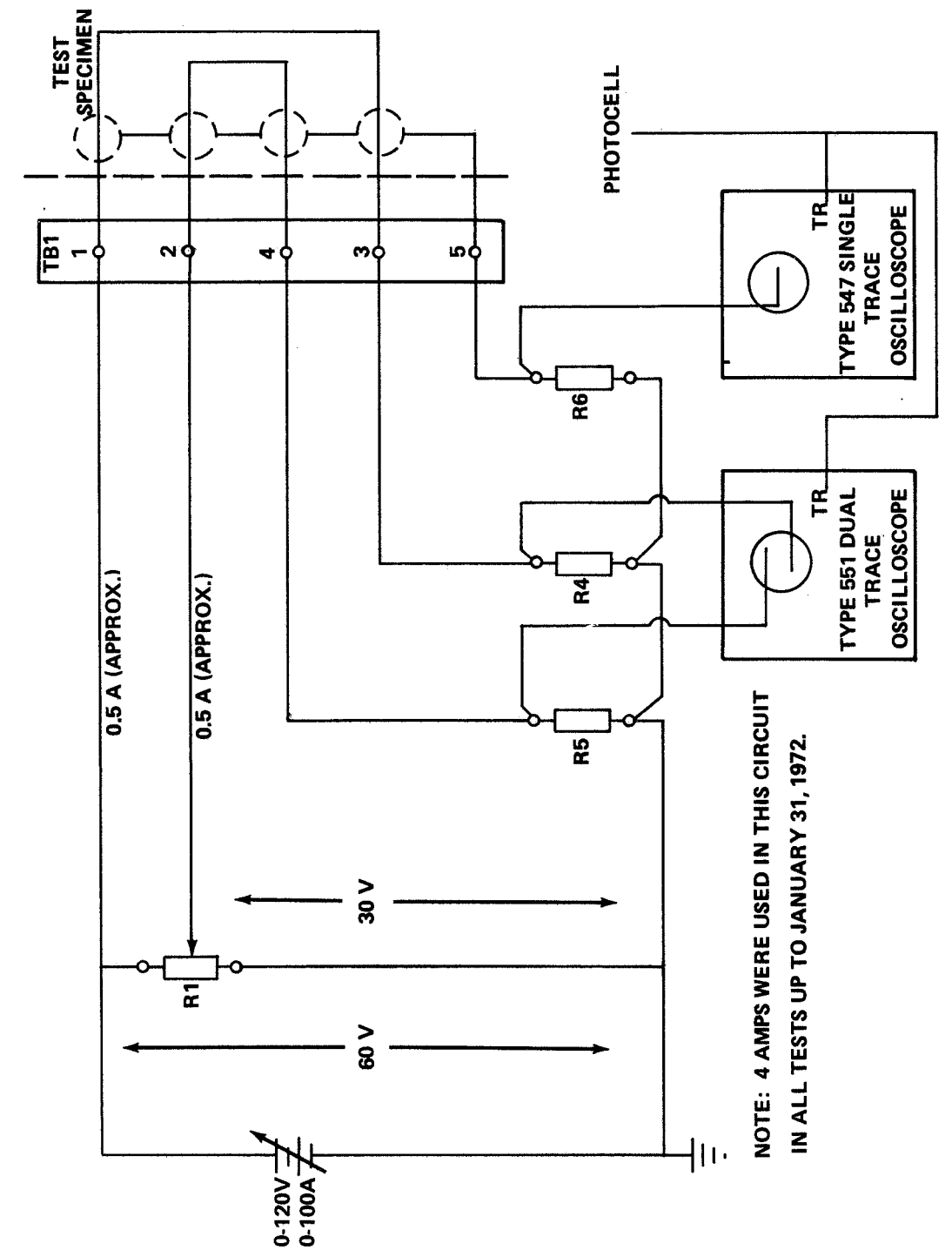

Figure A-9. Test monitor circuit for cable types 2 and 3.

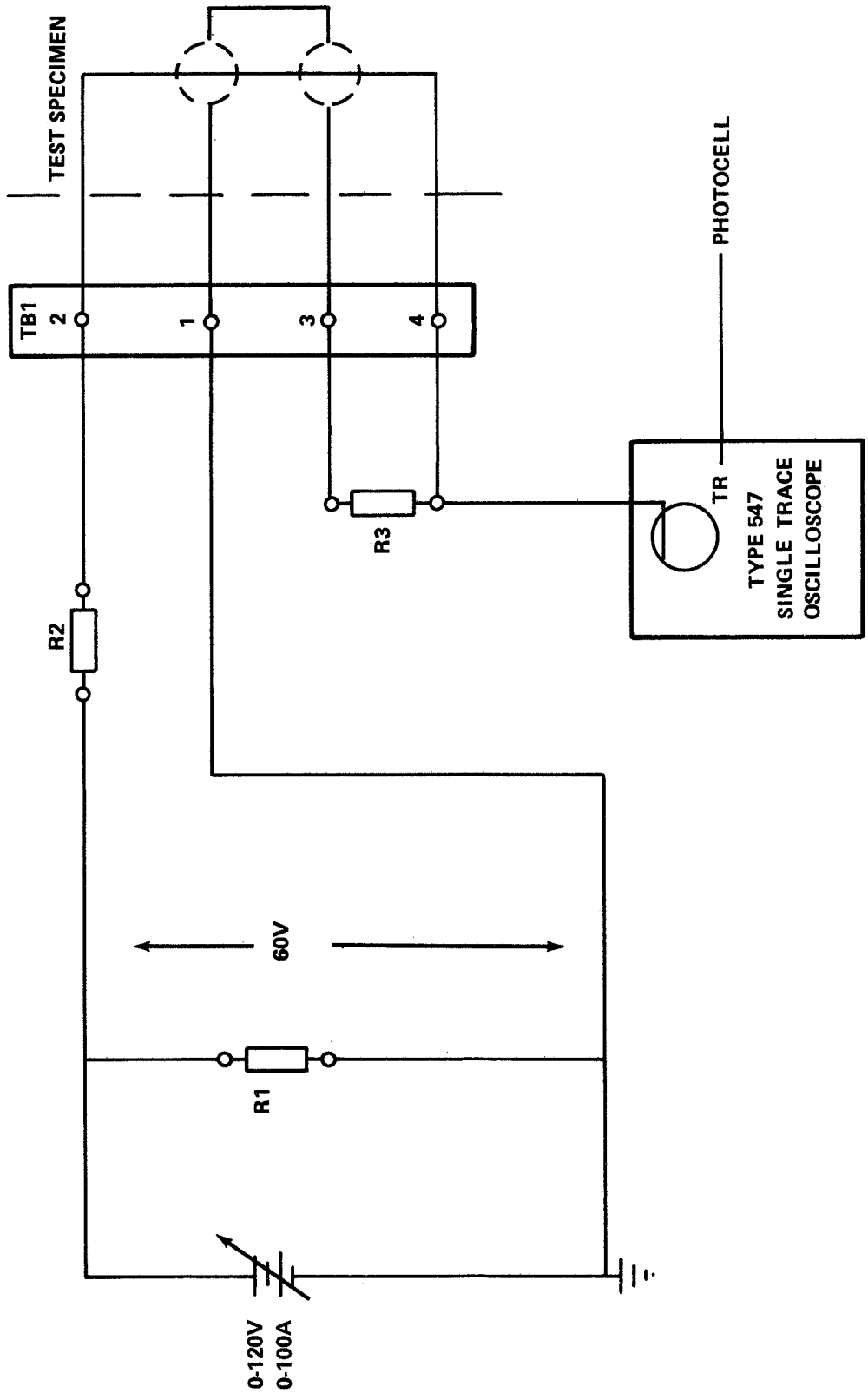

Figure A-10. Test monitor circuit for cable type 5.

e. Test Firings. The actual hitting of the test specimens with a simulated micrometeoroid (projectile) is a test firing. The test firing will utilize a light gas gun to fire projectiles of known size and density. The velocity of the projectiles will be determined by monitoring photocells along the tube of the light gas gun. The test specimen (target) will be placed in a vacuum chamber at the end of the tube. One photocell will be used to trigger oscilloscopes so that test specimen events may be recorded during impact and short duration thereafter.

f. Fact Test. After specimens have been mounted, a fact test will be performed before and after the test firing. The fact test will check for continuity of conductors and dielectric strength between mutually insulated conductors (shields included).

1. Continuity Check. Each conductor within the test specimen will be checked for continuity with not more than 4 amps flowing for not more than 30-s duration. Failures will be recorded.

2. Dielectric Check. The insulation of each test specimen will be tested between mutually insulated conductors (shields included) with 500 Vdc to detect less than 100 MΩ. Failures will be recorded.

g. Leakage Test. If the fact test after a test firing indicates that wires are shorted (shields included), a leakage test will be conducted to determine if the test specimen is sufficiently damaged to degrade the Skylab Mission. The leakage test will be conducted as indicated in Figure A-11. The power supply will be set to 28 Vdc with the switch in the "off" position. (At this time, the meter will read the applied voltage if a direct short is present.) The switch will be rotated through the six positions and any indicated voltage on the voltmeter will be recorded. Any voltage greater than 0.09 volt will constitute a failure. If no voltage is indicated, the procedure will be repeated with the power supply set to 32 Vdc. If the short remains, additional tests may be performed by the test engineers.

h. Test Evaluation. A test specimen that does not pass the leakage test after a test firing will be considered a failure. The test specimen will then be checked for broken or damaged strands. A change of state of any relay in test sequences 5 and 6 caused by a test firing will be considered a failure. The minimum energy level at which a failure occurs will be considered the ballistic limit of a cable type for evaluation purposes.

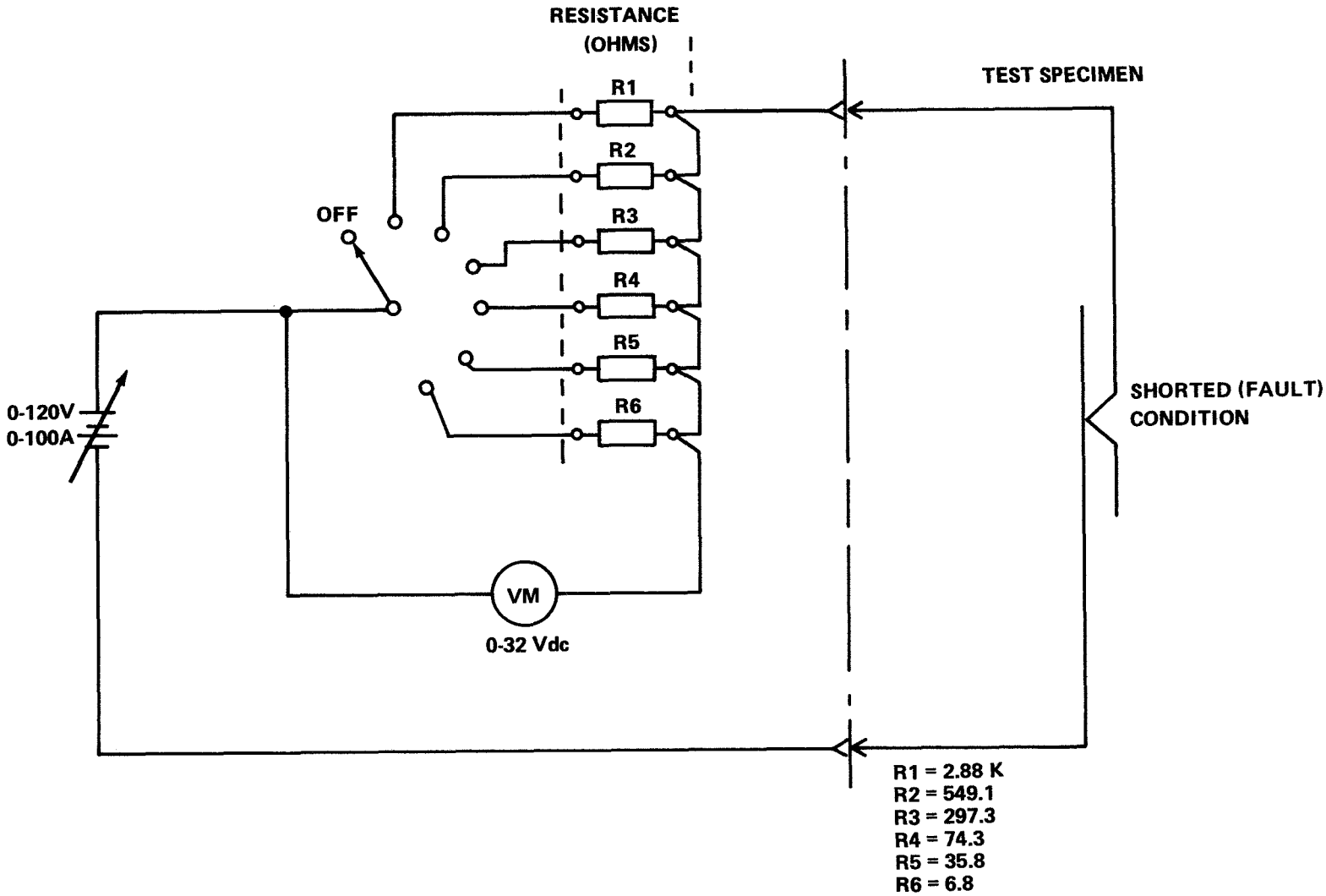

Figure A-11. Test circuit for current leakage test.

MICROMETEOROID CABLE TEST DATA SHEET

TEST SAMPLE: _____ NO. OF TEST: _____

DATE: _____ SSL CODE: _____

TIME: _____ CABLE FINE NO.: _____

TYPE TEST

DIRECT HIT ☐ POWER CABLE CURRENT ☐ SIGNAL CABLE RELAY ☐

INDIRECT HIT ☐ CABLE NO CURRENT ☐ _____ ☐

INSULATION TEST: BEFORE _____ AFTER _____

CHAMBER VACUUM: _____ TEST CIRCUIT DESIGN _____

METEORS: VELOCITY _____ DIMENSIONS _____

DENSITY _____ MATERIAL _____

SCOPE SETTING

TRIGGER SWEEP TIME: _____ TRIGGER POSITION: ☐

AMPLITUDE VOLT/CM: _____ TRIGGER SET: ☐

DC VOLT SELECTION: ☐ CAMERA LENS OPEN: ☐

	POWER SUPPLY		VOLTAGE/RESISTANCE						TEST CIRCUIT TERMINAL					
			1-3		1-7		2-4		2-7		3-7		4-7	
	VOLT	AMP	RES	VOLT	RES	VOLT	RES	VOLT	RES	VOLT	RES	VOLT	RES	VOLT
BEFORE														
AFTER														

RELAY CIRCUIT TEST DATA

	Before		After	
IND.	ON	OFF	ON	OFF
L1				
L2				
L3				

NOTE: L1 will be on until K1 is set which is the normal circuit condition.

REMARKS: _____

TEST DATA SHEET

(Cable Sample)

LEAKAGE TEST

DATE: _____

CABLE NO: _____

TEST NO: _____

SHORTED PINS: _____

TYPE OF SHORT: HIGH RES ☐ DIRECT ☐

VOLTAGE SETTING

28 Vdc ☐

SW. POS.	VM (Volts)	SAT	UNSAT
1			
2			
3			
4			
5			
6			

32 Vdc ☐

SW. POS.	VM (Volts)	SAT	UNSAT
1			
2			
3			
4			
5			
6			

(REF. Figure A-11 of Test Procedure)

REMARKS: _____

ADDITIONAL LOAD TESTS

Applied Volt	Load	Duration	Amps	Pins	Results

REMARKS: _____

EVALUATION TEST

_____

REMARKS

_____

APPENDIX B. READING OSCILLOSCOPE PICTURES

The following chart indicates the direction of movement of the oscilloscope traces under different conditions and refers to representative pictures.

Condition	Oscilloscope Traces		Representative Pictures
	30 V	60 V	
Short between 30 & 60 V coils	up	down	Test No. 3
Short between 30 V coil and ground or shield	down	slightly down	Test No. 45
Short between 60 V coil and ground or shield	No change	down	Test
Broken wire in 30 V coil	down	No change	Test No. 16
Broken wire in 60 V coil	No change	down	Test No. 52 both 30 V & 60 V broken

Note: Not all traces are clean direct current pulses. Some are mixed with heavy oscillations. Combinations of the above conditions produce a combination of the results.

George C. Marshall Space Flight Center
National Aeronautics and Space Administration
Marshall Space Flight Center, Alabama 35812, October 5, 1972
964-50-00-0000

REFERENCES

1. Meteoroid Environment Model – 1969 Near Earth to Lunar Surface. NASA SP-8013, March 1969.

2. Weidner, Don K. (Ed.): Space Environment Criteria Guidelines for use in Space Vehicle Development (1969 Revision). NASA TM X-53957, October 1969.

3. Naumann, R.J., Jex, David W., and Johnson, Clyde S.: Calibration of Pegasus and Explorer XXIII Detector Panels. NASA TR R-321, September 1969.

4. Naumann, R.J.: High Temperature Equation of State for Aluminum. NASA TN D-5892, August 1970.

NASA-Langley, 1973 —— 9 M450

"The aeronautical and space activities of the United States shall be conducted so as to contribute . . . to the expansion of human knowledge of phenomena in the atmosphere and space. The Administration shall provide for the widest practicable and appropriate dissemination of information concerning its activities and the results thereof."

—NATIONAL AERONAUTICS AND SPACE ACT OF 1958

NASA SCIENTIFIC AND TECHNICAL PUBLICATIONS

TECHNICAL REPORTS: Scientific and technical information considered important, complete, and a lasting contribution to existing knowledge.

TECHNICAL NOTES: Information less broad in scope but nevertheless of importance as a contribution to existing knowledge.

TECHNICAL MEMORANDUMS: Information receiving limited distribution because of preliminary data, security classification, or other reasons. Also includes conference proceedings with either limited or unlimited distribution.

CONTRACTOR REPORTS: Scientific and technical information generated under a NASA contract or grant and considered an important contribution to existing knowledge.

TECHNICAL TRANSLATIONS: Information published in a foreign language considered to merit NASA distribution in English.

SPECIAL PUBLICATIONS: Information derived from or of value to NASA activities. Publications include final reports of major projects, monographs, data compilations, handbooks, sourcebooks, and special bibliographies.

TECHNOLOGY UTILIZATION PUBLICATIONS: Information on technology used by NASA that may be of particular interest in commercial and other non-aerospace applications. Publications include Tech Briefs, Technology Utilization Reports and Technology Surveys.

Details on the availability of these publications may be obtained from:

SCIENTIFIC AND TECHNICAL INFORMATION OFFICE

NATIONAL AERONAUTICS AND SPACE ADMINISTRATION

Washington, D.C. 20546